Solar Array Suspension Mechanism

Final Design Report

for ATK Space

Presented by

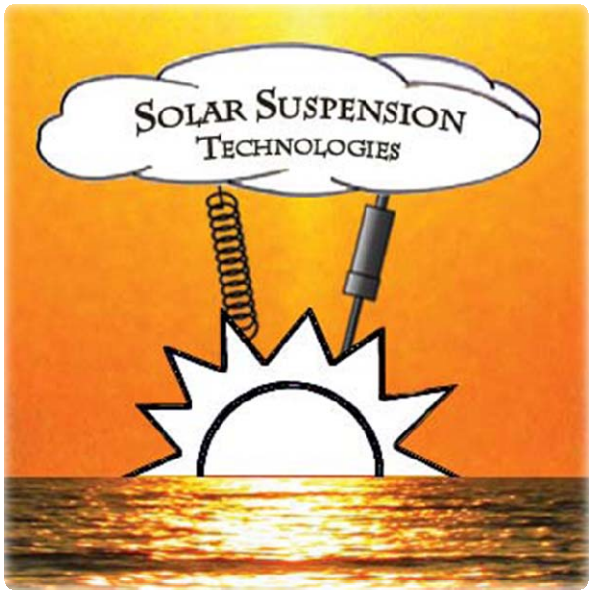

Alex Gould **Randon Kruse** **Jeremy Graul** **Patrick Barney**

sasm.polyteam@gmail.com

Mechanical Engineering Department

California Polytechnic State University

San Luis Obispo

June 3rd, 2010

Statement of Disclaimer

Since this project is a result of a class assignment, it has been graded and accepted as fulfillment of the course requirements. Acceptance does not imply technical accuracy or reliability. Any use of information in this report is done at the risk of the user. These risks may include catastrophic failure of the device or infringement of patent or copyright laws. California Polytechnic State University at San Luis Obispo and its staff cannot be held liable for any use or misuse of the project.

Table of Contents

List of Figures

List of Tables

Abstract

The purpose of this project is to improve the existing Solar Array Suspension Mechanism used by ATK Space for the manufacturing and testing of deployable solar arrays. The current system requires too much time to operate and has too many removable parts that may fall and damage the solar arrays. Through the design and verification process the team successfully constructed a quick connecting suspension mechanism that requires no tools to use and has no removable parts. The final design includes the existing force gauge and large adjustment bars used by ATK Space with the addition of a compression spring adjustment mechanism and a Socket Stud connection mechanism. The system was proof loaded at 300 lbs without any components yielding. The lowest factor of safety is about 5.2, which can be found on the Socket Stud. The estimated cost of the system is $2900, which is significantly less than the specified $8000 maximum cost.

Introduction

The purpose of this project is to improve the existing Solar Array Suspension Mechanism used by ATK Space, a premier aerospace and defense company located in Goleta, California, for the manufacturing and testing of deployable solar arrays. The current system requires too much time to operate and has too many removable parts that may fall and damage the solar arrays which would result in an expensive and time intensive repair by ATK Space. The team consists of four California Polytechnic State University, San Luis Obispo mechanical engineering students, Jeremy Graul, Alex Gould, Randon Kruse and Patrick Barney. The team developed improvements to both the connection mechanism and the suspension adjustments. This report documents the teams design, manufacturing and verification processes showing how the final design meets and exceeds the design specifications given by ATK.

1 Background

1.1 Purpose and function

The current Solar Array Suspension Mechanism (SASM) created and used by ATK functions not only as a mechanical support for the arrays, but as a leveling system. The deployment arm requires this support because it is not designed to support the weight of the solar panels in earth's gravity. In order to support the deployment arm, multiple suspension mechanisms are connected to the pivot points between each panel as seen in **Figure 2.** These support mechanisms keep the solar array panels level by a series of coarse and fine adjustment components, along with a force gauge. It is critical that the solar modules stay level in respect to one another during deployment in order to avoid high concentrated loads on the panels which could cause damage. The suspension mechanisms move with the arrays and are free to move on raised rollers on the off-loader track seen in **Figure 1** in the deployment direction, x and the lateral direction, y until the arrays are fully deployed. The lateral directional movements as seen are needed because the arrays do not offload in a straight chord. The individual components of the current SASM mechanism can be seen in **Figure 3**, along with the sub-categories in which these components fall into, which are used to organize the research.

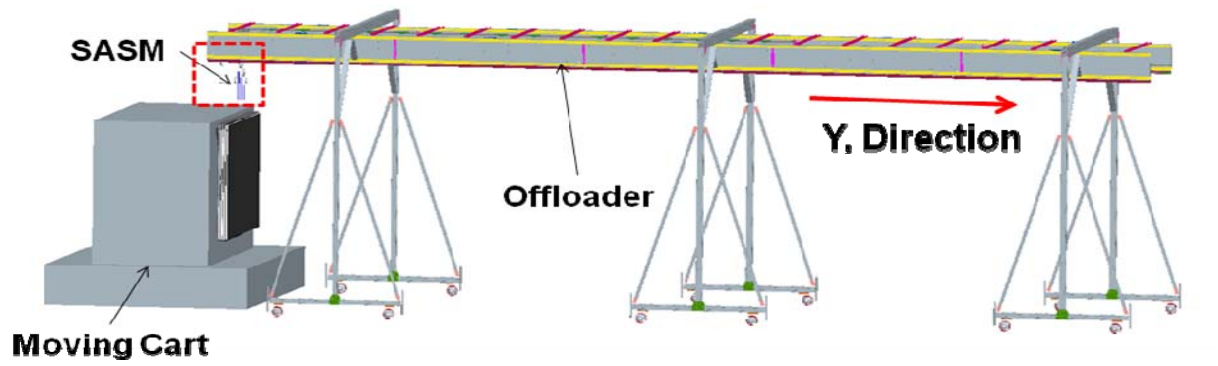

Figure 2. Offloader Assembly[1] containing Undeployed Solar Panels.

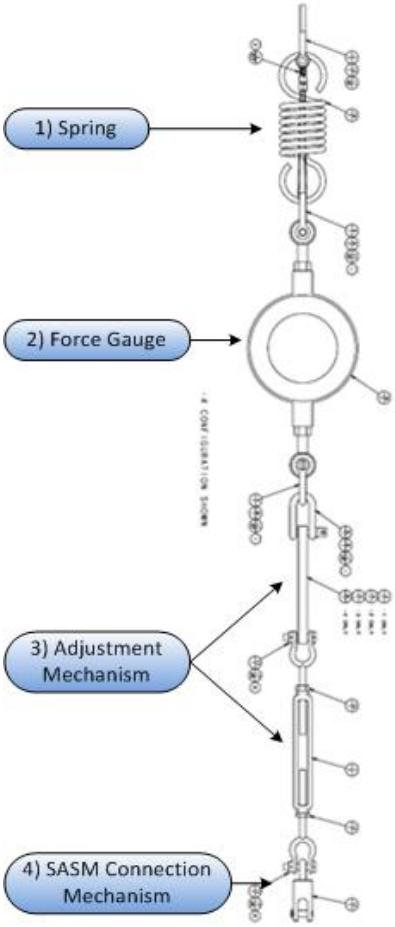

Figure 3. Current SASM configuration[1]

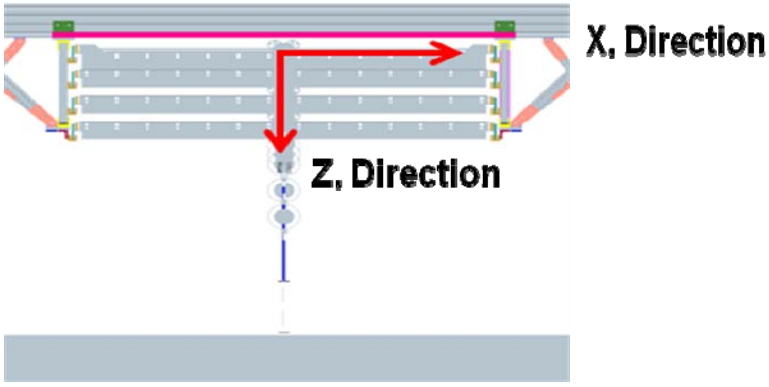

Figure 1. Off-loader configuration looking directly down the Y-axis

Current sub-categories and component include:

1. Spring
    a. Tension Spring
2. Force Gauge
    a. Analogue Ring Gauge
3. Adjustment Mechanism
    a. Turnbuckle
4. Connection Mechanism
    a. Ball Bearing Swivel and Clevis

[1] ATK Corporation

2 Components

2.1 Spring

Currently the SASM uses a mechanical helical spring in order to absorb loads caused by forced deflection. These deflections can arise during normal operation and testing. The joints located on the solar panel array are, by design, incapable of handling large internal stresses and moments. Thus even a small deflection can cause damage to the system. The force spring allows the SASM to change its height with only a small amount of force generated.

The current problems with the spring involve its physical size. The spring was sized to handle the global yield strength condition. In result, the spring is the widest component, which limits storage of the devices. Thus, any design improvement would concentrate on reducing the spring diameter. This is also a problem during deployment when the SASM need to be right next to each other. Not only does the helical spring limit how close each suspension mechanism can get, but the spring itself also has the potential of mechanically locking up with either spring located next to it.

A possible redesign consideration is a hydraulic or gas spring as seen in **Figure 4**. Hydraulic and gas springs can be made with much smaller outer diameters while maintaining similar yielding forces as a conventional helical stainless spring, such as the one currently used.

Figure 4. Hydraulic spring

Another possible redesign is known as a drawbar and can be seen in **Figure 5**. This method would replace the tension spring with a compression spring, and has a built in safety mechanism which could take the place of the metal wire in the current method which ties the force gauge directly to the overhead railing during max load testing.

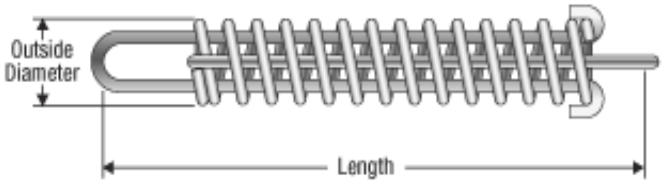

Figure 5. Drawbar Compression Spring

2.2 Force Gauge

The purpose of the force gauge is to quantify the weight distribution along the deployment arm, due to differences in vertical height of the solar arrays. Any variation in the z-direction causes a concentrated load on a specific joint, and increases the risk of damage.

A ring force gauge is currently being used to measure the load on the SASM. If the loads on all four mechanisms are not equal, a technician must adjust the turnbuckles to either lower or raise the mechanism, and redistribute the load so that it is even.

The current ring force gauge works well in the extreme temperature conditions seen by the SASM, since it is less prone to hysteresis, but the analogue gauge is difficult to read. It currently hangs about 8 feet above the ground and technicians must use ladders in order to elevate themselves high enough to read the small needle on the gauge. Also, when the solar panels are being tested in the insolated environment, it is impossible to read the loads on the panels during deployment since no one is stationed in the room.

There are many different ways to measure the tension force on an object. One method widely used in industry is with a tension load cell, which can be seen in **Figure 6**. The load cell itself uses a strain gauge to convert the small deflections in the material to an electrical signal. These signals are very small, so an amplifier is used increase the signal strength. These signals can be calibrated to accurately record the force on the suspension, which could then be sent to a computer or handheld display. The wireless transmission of data from the load cell to a user interface would decrease the time needed to level the system, and would allow for continuous data collection throughout deployment.

Figure 6. Force gauge with Wi-Fi data output

Figure 7. Spring force gauge

Another method of measuring tension force could be with a spring scale, which is shown in **Figure 7**. These springs are effective, but can have hysteresis problems, which cause them to be constantly calibrated. Also, using this type of spring would require a technician to look directly at the spring to take the reading, and reading a spring scale would be more difficult than reading the current ring scale.

2.3 Adjustment Mechanisms

The current adjustment system is broken down into either coarse or fine adjustments. The coarse adjustments utilize a combination of different length bars with holes drilled into them for screw attachments. The bars are inserted during the build of the apparatus, and are not modifiable while the panels are being hung from the SASM. While not in use, these large bars take up lab space, and are not convenient to change out, once the assembly is built. On the other hand, fine adjustments are used frequently between loads, and utilize a turn buckle to either raise or lower the panels by fractions of an inch. The same risks involving excess parts and components mentioned earlier apply to the adjustment mechanisms as well. The current turn buckle must be operated with a wrench, which increases the risk of damage on the panels due to tools being dropped.

One method of approach is to eliminate the distinction between coarse and fine adjustment components, and utilize a single component to meet both functions. An example of this could involve a locking, retractable cord as seen in **Figure 8**, or a system of pulleys**.** By having only one mechanism which controls the height of the panels without the use of tools, the time needed to operate decreases, along with the risk of damage.

Figure 8. Retractable Cord

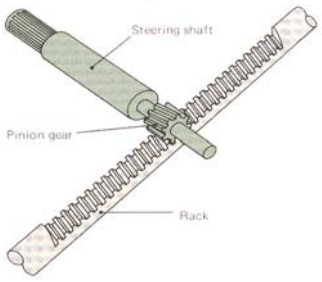

Figure 9. Rack and Pinion

Another method of approach would be to leave the coarse adjustment bars the way they are, since they are not used much, and focus on replacing only the fine adjustment components. One method of approach the team looked into includes replacing the turnbuckle with a rack and pinion as seen in **Figure**

9. But the rack and pinion can be broken down farther into a purely mechanical based system and an electric powered one.

The idea of bringing in electricity in order to remotely control fine adjustments has also been researched. If servos or linear actuators can be used to either move the SASM directly, or power a rack and pinion couple, the team would eliminate the risk of damaging the solar arrays completely, and also save the technicians the time spent on making fractional changes on precise instruments. But the added risk of running wires to each SASM is hypothesized to be problematic.

2.4 SASM Connection Mechanism

The current connection between the SASM and the solar array utilizes a swivel composed of modified eye bolt and screw in order to connect to the clevis, which is mounted to the panels. The SASM is first pulled down until the components line up with one another and then the screw is inserted through the eye bolt and clevis to make a positive, reliable connection. Even though this connection has been proven to be robust, it has its disadvantages. The amount of time required to screw and unscrew the eye bolt from the clevis are excessive and adds risk to the testing environment. The use of loose screws and additional tooling to adjust the screws increase the risk of damage to the solar panels. These excess parts are easily dropped, and if they crack a solar panel, the cost to replace them is significant.

In order to rid the assembly of the previously stated downfalls regarding the connection mechanism, the team looked into other methods of connection which were reliable, quick, and required no tools or loose parts to operate.

One promising device the group explored is the common day carabiner. The carabiner utilizes a metal loop with a screwed gate in order to quickly connect two components together in a single operation. As seen in **Figure 10**, carabiners can also have a locking mechanism to secure it from accidentally opening. This locking mechanism would make the connection between the SASM and panels easily verifiable and secure.

Figure 10. Carabiner

Another quick connect mechanism which does not require tools to operate is a grasper as seen in **Figure 11**. A specific use of this in our daily lives can be seen in the typical binder ring. These rings can be easily operated with a single hand, and can be integrated with a locking mechanism similar to that of a carabiner, in order to secure the connection. Another advantage of the binder ring is that less force is

required to pull the SASM down into place in order to connect to the clevis, since the connection location is lower on the ring than the current method.

Figure 11. Grasper and Binder Ring

3 Objectives

The overall goal is to design and build a Solar Array Suspension Mechanism which meets the needs of ATK engineering. The best way to meet the needs of the customer is to define quantifiable and measurable engineering specifications for each of the needs. The correlation between these needs and the developed specifications are weighted and related to one another through a process called Quality Function Deployment, and can be seen in **Appendix A**. Each of the customer needs is first given a weighted importance of how it ranks to the overall success of the project. After this is done, each developed specification is rated by how well it is able to test or quantify a given customer requirement. The sum of the products between the weighted importance of each requirement and the correlation ranking produces a weighted importance number for each specification. This tells the team exactly which specifications are vital to the success of the project, and therefore which problems to meet first.

This method was used to evaluate the customer requirements given by ATK for the SASM, and a condensed list of engineering specifications can be seen in **Table 1**. The specifications are grouped as either an overall system specification, or as a specific sub-system specification. By grouping the specifications in this way, it becomes clear which specifications are vital to the overall project, and which ones only pertain to a certain sub-system. In each group, the specifications and their corresponding quantifiable targets are listed. The tolerance of this target is then listed, and it can be seen that the target is often given as a maximum number. Following this, the risk associated with meeting the specification is listed as low, medium or high. Lastly, the table lists how the team will evaluate the specification. Analysis, inspections, or tests will be used to confirm compliance.

Table 1. Design Specifications

Overall System Specifications					
Spec #	Parameter Description	Requirement or Target (units)	Tolerance	Risk	Compliance
1	Number of Tools Required	0	Max	M	A
2	Quantity of Loose parts	0	Max	L	I
3	# of Actions Required to Operate	3 actions	Max	M	T
4	Visibility of Parts	All (High)	N/A	L	I
5	Width Dimensions	1.3 Inches	Max	L	I
6	Load Allowable	100 lb	+200lb	L	T
7	Cost	$8,000	Max	L	A
8	Weight	8 lb	Max	L	A,T
9	Temperature Range	-80 C to 50 C	Range	M	T
10	Clean Room Compatible	0 Intrusive Elements	Max	L	I,A

Specific Force Gauge Specifications					
Spec #	Parameter Description	Requirement or Target (units)	Tolerance	Risk	Compliance
11	Time To Check Force Gauge	5 seconds	Max	H	T
12	Force Gauge Resolution	1 lb	+/- 0.5lb	L	I

Specific Adjustment Mechanism Specifications					
Spec #	Parameter Description	Requirement or Target (units)	Tolerance	Risk	Compliance
13	Operation Time of Adjustments	30 Seconds	Max	L	T
14	Pitch Resolution	1/14"	+/-1/28	L	I

Specific Quick Connect Specifications					
Spec #	Parameter Description	Requirement or Target (units)	Tolerance	Risk	Compliance
15	Operation Time for Connecting	5 seconds	Max	M	T
16	Unload / Loading Deflection	3/4 inch	+/- 1/4"	M	I

In order for the overall system to be compliant with ATK requirements, there are 10 different specifications which much be met. The first and most important specification is that the new design must not require the use of tools. The current design uses screwdrivers and wrenches in both the quick connect and adjustment sub-systems, which adds excessive risk and time to the deployment operation. Furthermore, in order to stay compliant, the overall system must not rely on any loose parts such as screws, washers, or nuts. These loose parts can easily fall and damage the solar array, thus adding risk to the deployment procedure. A third overall system specification is the need to reduce the number of operations to three. As part of these three actions, the team is counting the current process of loading the SASM by pulling it down to the proper loading height as an action. This leaves only two actions, one for the quick connect and one for the possible adjustment. This is shown as a medium risk specification because the additional safety measures possibly needed on both connection and adjustment mechanisms may increase the number of operations beyond the specification. The forth global

specification is the high visibility of all components. By having all parts visible, it will be easier to confirm a positive connection between parts. The rest of the global specifications are all self explanatory and have a low risk of completion except for the broad temperature range specification. This extreme temperature range proposes problems when designing the force gauge, which will be discussed next.

When designing the force gauge sub-system, two more specifications must be kept in mind in addition to the global specs just mentioned. The more risky of the two is the specification to be able to make a force gauge measurement within 5 seconds during any point of any deployment. It is important for ATK to know if the weight distribution of the solar arrays becomes unbalanced during any part of the deployment. This shifted weight could be adding unwanted stress to the panel hinges, resulting in damage. But the only plausible method to make force gauge measurements during thermal testing when temperatures reach -80° is if the measurement is wirelessly transmitted to an operator who is out of the test environment. As stated earlier, the global specification of being able to operate in extreme temperatures proposes a high risk for battery operated components, and in particular, the force gauge.

In addition to the global specs, there are an additional two specifications specific to the adjustment mechanism. The first one is that it can be operated in less than 30 seconds. It is important that the operator can easily and successfully distribute the solar array's weight among all the suspension mechanisms in a timely manner in order to reduce risk. The more time the operator is up on the ladder, making adjustments, the greater the chance for something to get bumped or stressed. The second specification is that the fine adjustment pitch must be on the order of 1/28" in order to fine tune the displacements enough to eliminate unequal weight distribution.

Lastly, the quick connect sub-system has an additional two specifications which need to be discussed. In order for the quick connect to be considered "quick", the team placed a time limit of 5 seconds onto the operation. This time includes any additional steps necessary to insert safety locks, which is why there is medium risk associated with meeting this specification in full. The second specification is relevant to the loading and unloading steps of the solar arrays to the quick connect. Currently, in order to load the SASM, the mechanism must be pulled down an inch in order for the hole in the u-loop to be coaxial with the clevis hole. Due to the large spring constant, it is difficult to pull down the mechanism any further than an inch, which means that the quick connect must be able to connect to the panels without excessive loading to position it correctly.

For further detail on how the team has evaluated the current design and where improvements can be made, refer to the QFD, house of quality in **Appendix A**.

4 Method of Approach

The project presented is an excellent example of a product that can be reengineered using the classic engineering design process. This method of engineering is often described as an iterative decision making process that can be outlined by **Figure 12**. This process was started prior to our group receiving this project when ATK concluded that there was a deficiency within their manufacturing line where an improvement could be made. As soon as the project was presented to the team, the engineering process continued at full speed.

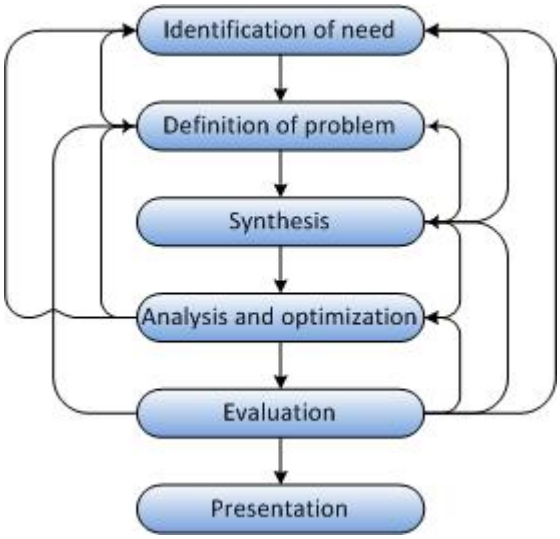

Figure 12. Design Process

The second step of the design process is defining the problem. The specifications aforementioned were created in partnership with ATK to better understand the requirements of the project in order to confirm the spectrum of the project. This portion of the design process specifically requires background information on existing devices used for this and similar applications, and the objectives and goals for this project. Iteration of the research, objectives and specifications may need to take place in the future with constantly evolving ideas. This is true for each step of the design process to be mentioned.

The next section of the engineering design process is called synthesis. This involves the creation of ideas and prototypes. Concept generation techniques are used to create a number of possible solutions. Sketches and simple analysis help reduce the number of solutions to three to five prominent concepts. Once the final design is narrowed down to one or two designs, CAD is used to generate 3-D models to help with further analysis and decision making. Throughout this process, prototypes can be produced in order to determine feasibility and practicality.

The next step to the design process is the iteration process of fabrication of prototypes, analysis and optimization of said prototypes, and evaluation of the design. This process is repeated multiple times until the most ideal product is produced. It is important to keep ATK in close communications with the

team throughout the design process so no surprises or miscommunication can occur. After the most ideal device is created and tested rigorously, the final step of the engineering design process will be completed and a final project report and presentation of the product.

5 Design Development

After extensive research of existing springs, quick connect, adjustment, and force gauge components, team members created conceptual models of ideas which had potential of meeting the engineering specifications. In order to distinguish which of these concepts conformed to the engineering specifications the best, the team constructed a decision matrix for each of the four sub-categories. The matrices quantify the improvement of each concept over its existing design. This was done by awarding the concepts a +1 if it met a specific specification better than the existing, a -1 if the concept was less likely to meet a specification, or a 0 if both existing design and concept meet the specification equally. But since certain specifications are more important to the overall success of the project, a weight was added to each specification in order to better quantify its importance. This weighted number was then multiplied by the initial score of either 1 through -1, and the sum of the weighted scores was then used to compare the concepts to one another.

The following four sections break down the component concepts into four major sub-systems, spring, force gauge, extension mechanism, and connection mechanism.

5.1 Spring

The current tension spring's diameter is on the large side, and sometimes gets in the way when storing the panels in the stacked position. In addition to this, since the tension spring does not have a max load safety limit built in, an additional metal wire must be used during maximum loading tests in order to not damage the spring. Out of the two concepts generated, the compression spring was the only one which showed a positive improvement over the current design in the decision matrix shown in **Table 2**. This will also be the only design which will be detailed in this section.

The weight factors associated with the specifications make certain ones more important than others, based on their impact on the overall success of the system. For the spring, the width, load allowable and clean room compatibility are all weighed heavily with a factor of 5. This is because each of these specifications directly affect the functionality and feasibility of the spring. If the spring is too wide, it

won't be able to store in the stacked position, deeming it unusable. Likewise, if it doesn't meet the load requirements, or utilizes incompatible materials such as grease, the spring will become a hazard to the work environment. The remaining two specifications of weight and cost are weighed so low because they do not have much of an impact on the success of the new spring design.

Table 2. Spring Decision Matrix

		Die Compression Spring		Gas Spring		Current Design	
	Weight Factor	Rating	Weighted Rating	Rating	Weighted Rating	Rating	Weighted Rating
Width Dimension	5	0	0	1	5	0	0
Load Allowable	5	1	5	0	0	0	0
Clean Room Compatible	5	0	0	-1	-5	0	0
Weight	2	0	0	-1	-2	0	0
Cost	1	0	0	-1	-1	0	0
			5		-3		0

One primary benefit to using a die compression spring over the contemporary tension spring is that it has a built in safety for the max load. When the max load is applied on a tension spring, the spring coils are more vulnerable to yielding if they are pulled beyond their elastic limit. On the other hand, if the compression spring is loaded beyond its yield limit, it will bottom out on itself. As this load gets increasingly higher, there is a chance of buckling, but it is possible to build a support around the spring in order to avoid buckling.

5.2 Force Gauge

One of the main limitations of the currently used ring force gauge is that it uses an analogue display that must be viewed on the actual suspension. The gauge itself is very robust and doesn't have any hysteresis problems, so the only improvements that can be made are to the display. Out of the two concepts generated for the force gauge, none of the options showed an improvement to the existing design, as shown in **Table 3**.

The reason why the load cell and spring scale scored so poorly is because they failed to improve upon any of the highest ranking specifications. These specifications corresponded to the weight factor of 5 and directly affect the functionality of the gauge. The width of the force gauge is important because if it exceeds the max width of 1.3 inches, it will not attach to the panels in the stored position. The load

allowable affects the functionality of the complete system since all the sub-systems are connected in series. If the force gauge yields, the entire SASM becomes nonfunctional, and a hazard to the work environment. The temperature range is weighted so highly because the gauge needs to survive in -80°C environment or the added advantage of real time data collection becomes compromised. The second highest weighted specifications, corresponding to the weight factor of 4, are defined as specs which measure the ease of reading the force gauge. These specs are ranked relatively high because this is where the current analogue display needs the most improvement. The remaining specifications are weighted low because they do not affect the overall success of the project.

Table 3. Force Gauge Decision Matrix

		Load Cell		Spring Scale		Current Design	
	Weight Factor	Rating	Weighted Rating	Rating	Weighted Rating	Rating	Weighted Rating
Time To Check Force Gauge	4	1	4	0	0	0	0
Width Dimensions	5	-1	-5	1	5	0	0
Visibility	4	1	4	-1	-4	0	0
Load Allowable	5	0	0	-1	-5	0	0
Force Gauge Resolution	2	1	2	-1	-2	0	0
Cost	1	-1	-1	1	1	0	0
Weight	2	-1	-2	0	0	0	0
Temperature Range	5	-1	-5	-1	-5	0	0
			-3		-10		0

Research was conducted to find a load cell which would be compatible in both the thermal testing room and the standard clean room, but the conclusion reached at the end was that a load cell would not improve the existing design. The additional components necessary in order to power and wirelessly transmit the data can be seen in **Figure 13** and would make the overall assembly bulkier and possibly even more time consuming than the original design. Our research concludes that even though it is possible to purchase a cryogenic load cell which meets the extreme temperature conditions, it is not possible to have a functioning wireless transmitter and battery in the thermal testing environment without external heating. This means that a flexible heater would need to wrap around all the thermally sensitive components during thermal testing. In addition to thermal considerations, the team ran into issues in how to properly power the system. If a rechargeable battery is used to power the wireless

transmitter and heating element, it would need to be recharged prior to testing. This would require a technician to climb up the ladder before every test to install four new batteries and power up the load cells. The only other alternative would be to power the system directly from an electrical cord. But this option would require the team to develop a method to keep the four required electrical cords from interfering with the solar panels or getting caught in the railing during deployment.

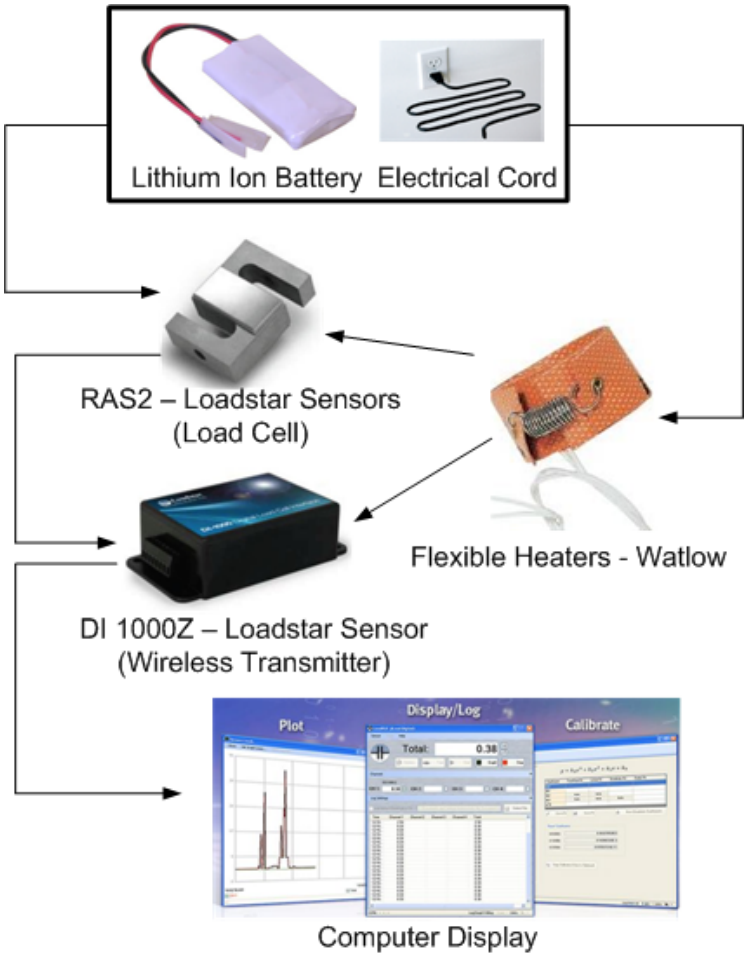

Figure 13. Required Load Cell Configuration

5.3 Adjustment Mechanism

The current adjustment mechanism cannot be operated without tools, and takes about 5 steps to loosen both safety nuts, raise or lower the turnbuckle, and then retighten the safety nuts. The extensive amount of time needed for adjustment, along with the added risk of loose parts and tools, allow for improvements in several key specifications. Furthermore, the current adjustment mechanism is limited in travel to the size of the turnbuckle, and any adjustments needed beyond this range require the disassembly of the SASM. Three designs were created, as shown in **Table 4,** each with their own advantages and disadvantages. In the end, the compressed spring adjustment method improved on the existing design the most.

In order to explain the added benefits or shortcomings of each design, it is necessary to understand the weight factors associated with each specification, and the reasoning behind the numbers. A weight factor of 5 was given to the specifications which directly affect the feasibility or risk associated with using the conceptual adjustment mechanisms. As stated in the objectives, additional tools and loose parts add risk to the operation and must be removed. In addition, the compatibility with the clean room and high load allowable specifications are weighed so high because the concept can't be considered for use if it can't meet these. The last specification which directly affects the feasibility of the design is the width. A wide adjustment mechanism will make the stacking of the panels very difficult. The second highest weighted specifications, correlating to a factor of 4, correspond to the amount of time or effort needed to properly adjust the mechanism. The operation time of the current turnbuckle is relatively high, and is where the most improvements can be made. In addition to improving the design to decrease the overall adjustment time, the number of actions and the range in which the adjustments can be made also affect the efficiency. If the adjustment can have a high enough range to eliminate the need for both coarse and fine adjustments, time will be saved in disconnecting the SASM for large changes. One medium weighted specification is the pitch resolution. A smaller pitch would allow the operator to more easily and accurately level the panels, but would also lengthen the amount of time needed to complete the operation. Both of these functions need to be balanced in order to design the most efficient adjustment which is both accurate and quick. One final specification worth mentioning is the minimum height requirement. Even though it has a weight factor of 2, it is important to keep in mind when trying to design for the shortened thermal testing room. The current design does not sufficiently account for the shortened roof, and utilizes makeshift turnbuckles in order to shorten the SASM enough to fit. All of the specifications aforementioned can be seen in the table below.

Table 4. Adjustment Mechanism Decision Matrix

		Compressed Spring Adjustment		ACME Threaded Screw		Screw Jack		Current Design	
	Weight Factor	Rating	Weighted Rating	Rating	Weighted Rating	Rating	Weighted Rating	Rating	Weighted Rating
Operation Time	4	1	4	1	4	1	4	0	0
Required # Of Actions	4	1	4	1	4	1	4	0	0
No Tools Required	5	1	5	1	5	1	5	0	0
Small Width Dimension	5	0	0	0	0	0	0	0	0
High Load Allowable	5	1	5	0	0	0	0	0	0
Clean Room Compatible	5	0	0	0	0	-1	-5	0	0
Pitch Resolution	3	-1	-3	-1	-3	-1	-3	0	0
No Loose Parts	5	1	5	1	5	1	5	0	0
Low Cost	1	-1	-1	-1	-1	-1	-1	0	0
Low Weight	2	-1	-2	-1	-2	-1	-2	0	0
Manufacturability	3	-1	-3	-1	-3	1	3	0	0
Range	4	1	4	1	4	0	0	0	0
Minimum Height	2	1	2	1	2	-1	-2	0	0
			17		12		8		0

5.3.1 Compressed Spring Adjustment

The compressed spring adjustment utilizes the extra space inside the core of the suspension spring to store the extra thread of the adjustment. The biggest difference between this design and the existing design is that it utilizes a compression spring instead of a tension spring. But by doing this, a support canister has to be built to transfer the tension load seen in the SASM into a compressive load for the spring. This canister can be seen in black in **Figure 14**, and consists of two cylindrical plates screwed onto a tube to make an enclosure. This enclosure can be used to support the spring during max load testing in order to keep it from buckling.

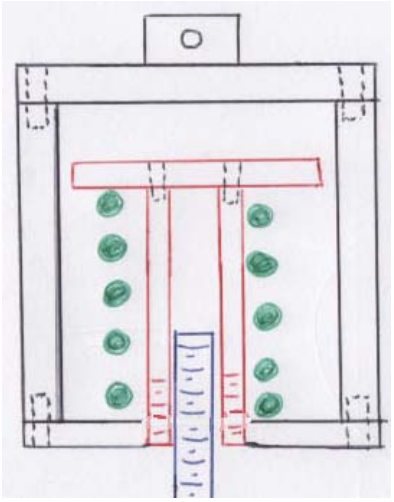

Figure 14. Compressed Spring Adjustment

The way adjustments are made with this concept is by simply rotating the threaded bar seen in blue in **Figure 14** such that it either rises into or retracts out of the threaded collar seen in red. By storing the extra thread, it has the ability to condense the overall length of the design to make it more feasible for the thermal testing room.

This concept scored the highest in the decision matrix because it was successful in either meeting or improving on all the highest weighted specifications. It is capable of making fine adjustments without the use of tools or loose parts, while efficiently utilizing space to make the overall SASM more feasible in the thermal testing room. Even though the advantages outweigh the disadvantages, the manufacturing process of this concept is going to be a lot more time consuming than the existing design.

5.3.2 ACME Threaded Screw with Collar

The second highest scoring adjustment mechanism is similar to the Compressed Spring Adjustment because it also uses the empty space inside the core of the spring to store excess thread. The assembly as seen in **Figure 15** would attach the support spring to a custom collar. The collar is then used to adjust the total length of the suspension mechanism while simultaneously storing the unused thread within the core of the support spring. In order to give the collar the freedom to rotate, the top of the spring will be attached to a swivel and the bottom of the thread will have its rotational freedom fixed.

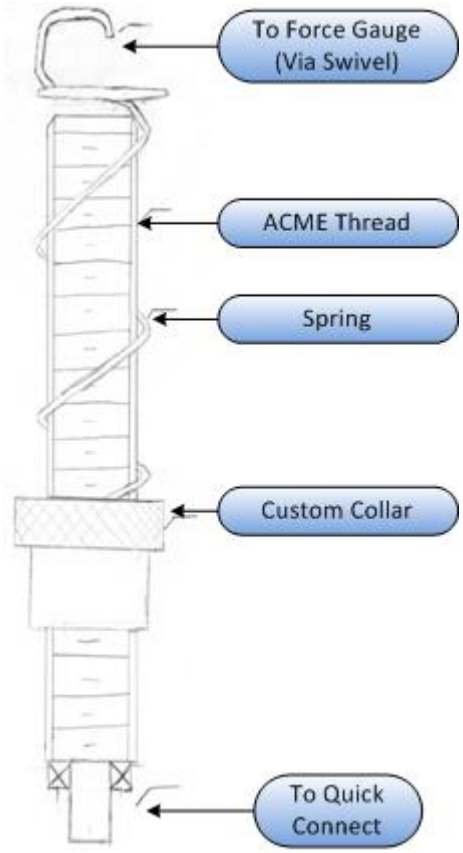

Figure 15. ACME Thread Sketch

This design's width would be about the same as the spring in the current suspension system, thus reducing interference problems before deployment. Furthermore, storing the extra thread inside of the spring has the benefit of significantly reducing the minimum length of the suspension system potentially mitigating the height constraint issue in the thermal testing room. Finally, different lengths of rod could be used in the same way that the current course adjustment bar functions in the current suspension system.

Although the concept improves the existing design, this system still has a number of disadvantages. The custom collar will need to be manufactured. The custom collar will need to have a

locking mechanism built into it as well as a groove so that it may attach to the spring. The other major disadvantage is that large lengths of unused thread could potentially work their way in between the coils and lock.

5.3.3 Screw Jack

Another method of making precise adjustments is by using a screw jack similar to that seen in **Figure 16**. An exterior knob would be used to move an internal rack up and down. This concept scored relatively high in the decision matrix because it is able to make fine adjustments without the use of tools or loose parts.

Figure 16. Screw Jack

Although the concept improves the existing design, there are a few disadvantages. First off, the manufactured component does not come with an internal locking mechanism, which means that one would have to be machined to prevent the jack from potentially elongating while under load. Secondly, the internal gearbox may require grease, and as a result, not be appropriate for the clean room.

5.4 Connection Mechanism

The current method of using a clevis and u-loop to connect the SASM to the solar arrays is time consuming, requires an excessive amount of actions, and adds risk to the operation by the use of tools and loose parts. All of the proposed designs were able to improve on the three previously mentioned specifications, and showed positive improvements to the existing design overall. From the decision matrix shown in **Table 5**, the carabiner was shown to best improve the existing design, while the rest of the concepts scored relatively similarly, except for the Push Pin Lever, which was unable to show a positive connection, unlike the other designs. The five concepts with the most potential are discussed below.

To aid in the decision matrix utility, each specification has a weight factor which was determined by its relative importance to the other specifications. No tools required and no loose parts both received a weight factor of 5 since these two factors determine the success of the device. Eliminating loose parts would greatly reduce the risk associated with installing the solar arrays as well as simplify the installation process. High load allowable has a weight factor of 5 since the failure of SASM device would lead to solar array damage and an unsafe work environment which are both unacceptable. The

operation time for connecting the panel and the number of actions required are two important specifications that would greatly improve the device but do not determine the total success of the project, so they received a weight factor of 4. The number of actions required is defined by the number of steps needed to complete the operation. The current steps required are pulling the SASM down to align with the clevis, placing the bolt through the holes, placing the nut on to the bolt and then tightening the nut to total four actions required. The new design would like to implement a connection procedure containing less than 3 actions. The remaining specifications are weighted relatively low because they do not affect the overall success of the project. It is important to note that the positive connection specification was defined by the number of senses used to verify connection such as visual and auditory. The six concepts with the most potential are discussed below.

Table 5. Connection Mechanism Decision Matrix

		Carabiner Mechanism		**Pneumatic Connection Push to Lock**		**Swivel - Nub**		**Current Design**	
	Weight Factor	Rating	Weighted Rating	Rating	Weighted Rating	Rating	Weighted Rating	Rating	Weighted Rating
Operation Time for Connecting	4	1	4	1	4	1	4	0	0
Number Of Actions Required	4	1	4	1	4	1	4	0	0
No Tools Required	5	1	5	1	5	1	5	0	0
Positive Connection	3	0	0	1	3	0	0	0	0
High Load Allowable	5	0	0	0	0	0	0	0	0
No Loose Parts	5	1	5	1	5	1	5	0	0
Low Cost	1	1	1	-1	-1	-1	-1	0	0
Low Weight	2	0	0	0	0	0	0	0	0
Manufacturability	3	1	3	-1	-3	-1	-3	0	0
Excess Load Required	2	-1	-2	0	0	0	0	0	0
			20		17		14		0

		Socket Stud		U - Loop		Push Pin / Lever		Current Design	
	Weight Factor	Rating	Weighted Rating	Rating	Weighted Rating	Rating	Weighted Rating	Rating	Weighted Rating
Operation Time for Connecting	4	1	4	1	4	1	4	0	0
Number Of Actions Required	4	1	4	1	4	1	4	0	0
No Tools Required	5	1	5	1	5	1	5	0	0
Positive Connection	3	0	0	0	0	-1	-3	0	0
High Load Allowable	5	0	0	0	0	0	0	0	0
No Loose Parts	5	1	5	1	5	1	5	0	0
Low Cost	1	-1	-1	-1	-1	-1	-1	0	0
Low Weight	2	0	0	0	0	-1	-2	0	0
Manufacturability	3	-1	-3	-1	-3	-1	-3	0	0
Excess Load Required	2	0	0	0	0	0	0	0	0
			14		14		9		0

5.4.1 Carabiner

The carabiner is shown to improve on the existing design the most. This is because it can quickly and positively connect an I-Hook to the SASM without the use of tools or loose parts. It is also easy to manufacture, since it can be purchased from a variety of manufacturers and requires no additional machining in order to assemble it to the rest of the SASM. The only downside of the carabiner is that an excessive amount of force is needed to pull down the spring in order to load the eye-bolt into the carabiner. A preliminary shear stress analysis of a carabiner under a 300 lb load can be seen in **Appendix F**.

5.4.2 Pneumatic Hose Coupling

Another high scoring idea considers the use of a pneumatic air hose quick connect coupling. This device, as shown in **Figure 17**, is extremely user friendly and easy to operate. The specific hose connect studied has a push to connect feature. By simply placing the female end over the male clevis and pushing together, the two pieces lock together. The quick connect works by the use of ball bearings that are capable of locking into a groove on the male connection point. The ball bearings lock into place by the outer sheath sliding down, trapping the ball bearings in with a smaller diameter ring inside the sheath. To release the male terminal from the female, the operator pulls the sheath back until it disconnects.

This device scored well in the decision matrix because it met all the heaviest weighted specifications, such as the elimination of tools and loose components, and it is the only concept that improves the ability to show a positive connection due to its combination of both visual and audible connection qualities. Also, the general ease of use of this device is a huge positive for the success of this concept.

Shear stress analysis and ball bearing contact farces of the pneumatic hose coupling can be seen in **Appendix H.** Analysis on the store bought pneumatic hose connection indicates extremely high pressure points where the ball bearings contact the male clevis that would cause failure at the surface. Since this would be unacceptable, this concept is no longer being pursued.

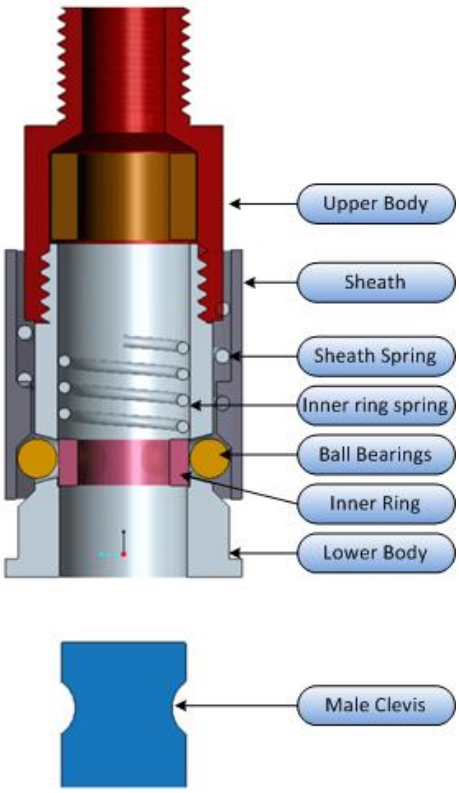

Figure 17. Pneumatic Hose Coupling Assembly Cross Section

5.4.3 Swivel Nub

Another promising concept is the "Swivel-Nub", as seen in **Figure 18**. The panel connection piece is screwed into the panels, and is held stationary in the vertical position. In order to connect the SASM onto this connection piece, the swivel component is brought down such that the extrusions of the panel connection go through the slots in the swivel, and then the swivel is rotated in the counter clockwise direction to lock it in place. The gravitational force on the panels will keep the nub of the panel connection piece inside the locking groove of the swivel, until the swivel is manually pulled down and twisted in the clockwise direction to disengage.

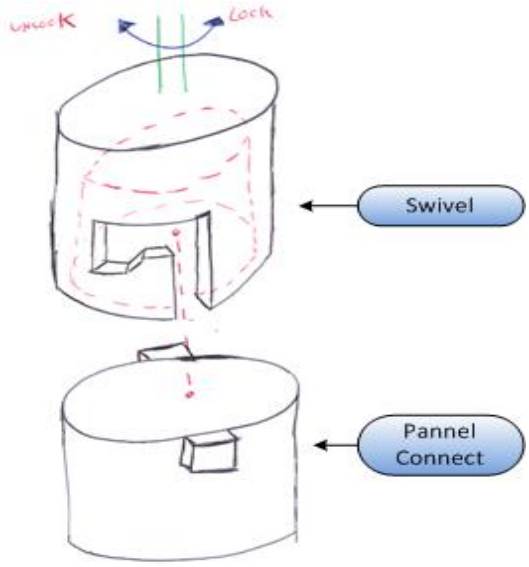

Figure 18. Swivel Nub

The Swivel Nub concept tied for third in the decision matrix due to its ability to greatly improve all the heavily weighted specifications, such as the elimination of tools and loose components, and the reduction of steps and time to operate. Preliminary shear stress calculations of both the swivel and panel connection can be seen in **Appendix I.**

5.4.4 Socket Stud

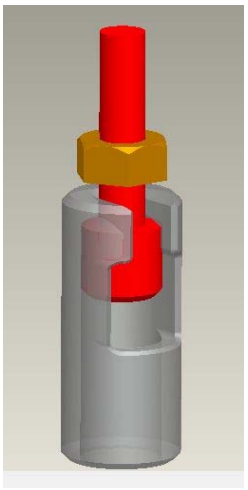

Figure 19. Socket Stud

Another quick connect concept that has potential is called the Socket Stud and is shown in **Figure 19**. This concept uses a mechanism closely related to a bike brake cable and how it is attached to the brake lever. At the end of a shaft (what would be the cable on a brake cable) is a larger diameter cylinder that can slide into a socket. When the shaft is raised, a ridge prevents the shaft from sliding out of the socket. The shaft could then be locked into place by a safety nut by threading it down to the body of the socket, as shown in **Figure 19** by the brass colored nut. The mechanism can be compact and can be designed to be no more than $3/4^{ths}$ in diameter. This design gives the user a sturdy, positive connection that is easy to verify. Initial calculations which show that this design is able to support the max load without yielding can be seen in **Appendix J.**

5.4.5 U Loop

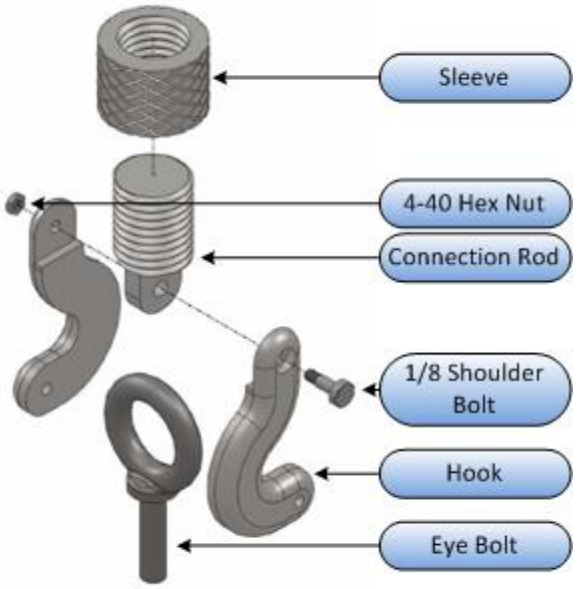

Figure 20. U-Loop Concept Assembly

Another potential concept uses two hooks to close around an eyehook, and can be seen in **Figure 20**. The hooks are pressed close to each other and rotate about a pin. To close the mechanism, there is a threaded sleeve that can be screwed down over the top of the hooks, locking them closed around the eyehook. This solution requires no tools and has a positive connection. Once the hooks are locked in place and loaded, the force of the load will press the hooks together, further locking them in place. To disengage the hooks just unscrew the sleeve and pull down on the suspension. The hooks can be easily separated at this point and the solar arrays are no longer attached.

The U-Loop connection mechanism scored fairly well in the decision matrix because if its simplicity and its strength. Analysis was done on the hooks and shoulder bolt using the Maximum Shear Stress Theory. The minimum yield strength for the hooks to support a 300 lb weight is 16.4 kpsi, which can be greatly

exceeded with most aluminum alloys. The minimum yield strength required for the pin 32.6 kpsi which can be easily met by most carbon steels. The stress analysis calculations can be found in **Appendix K**.

5.5 Ergonomic Tests

In order to narrow down the initial design concepts, an ergonomics test was completed for each design. This test was used to really feel and understand each design because none of the concepts really stood out from the decision matrix. Each concept considered was either purchased or rapid prototyped at full scale. The designs were then attached to the frame with the top section suspended by a spring to simulate the reactions of the suspension rod. The bottom section of the mechanism was mounted to the bottom of the frame to simulate the rigid solar arrays prior to deployment. **Figure 21** below shows the test fixture with each connection method attached.

Figure 21. Ergonomic Test Set Up

The connection mechanisms were tested by about twenty different people, including the SASM Team. The users were asked to connect and disconnect each mechanism and rank each mechanism on a numeric scale from easiest to hardest to use. The results of the test are shown below in **Figure 22**.

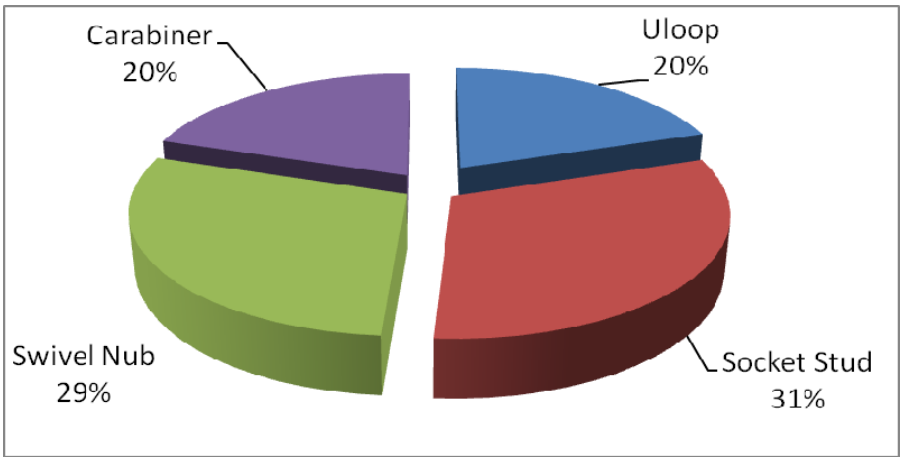

Figure 22. Ergonomic Test Results

The top designs were the Socket Stud and the Swivel Nub. Although the carabiner and U Loop were not that far behind, the SASM Team felt that the auto-locking features of the Swivel Nub and Socket Stud really set them apart from the others. Due to the low cost of each of these mechanisms, the SASM team manufactured both the Swivel Nub and Socket Stud and did strength and thermal testing on each design before making a final decision on which design to utilize in the final assembly.

6 Manufacturing

6.1 Machined Swivel Nub

Initial ergonomic testing and analysis narrowed down the final design to two quick connect designs and a combined adjustment and spring mechanism. Early issues with the manufacturing process of the swivel nub urged the team to look into casting several of the components. The manufacturing process of both the machined and casted swivel nub are discussed below, followed by the manufacturing process of the socket stud and adjustment mechanism.

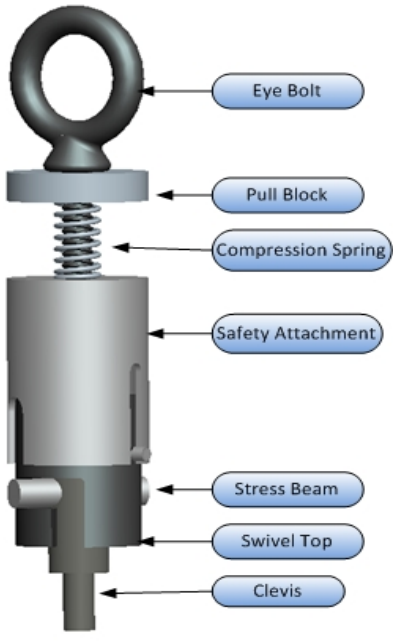

Figure 23. Swivel Nub Manufacturing

The manufacturing of the finalized swivel nub seen in **Figure 23** was more time consuming than planned and the machining was not trivial. The assembly consisted of five machined components, three being aluminum and two being steel. All of the work was either done on a lathe or a mill, and the total machining time is estimated to be around 4 ½ hours. The

manufacturing process of the swivel top took about 2 hours itself, and the steps taken to manufacture it are worth reviewing.

The first step in machining the Swivel Top was to drill the through hole for the ¼-20 tap. This was done by placing a one inch diameter stock aluminum rod on the lathe and drilling the minor diameter of Ø.188" into it. After this, the inner cavity was bored out by first using a ½" mill to drill to the correct length, and then using a boring bar to create the flat end condition of the inner cavity. This step finalized the work on the lathe, and the un-parted aluminum bar was brought over to the fourth axis mill to do the rest of the cuts. It was important to not part the aluminum to length since a lot of extra metal was needed to provide enough metal to clamp onto in the mill chuck.

The forth axis mill was set up such that the swivel top axis is horizontal to the table. The forth axis was rotated for convenience to 0 degrees and a ¼ inch end mill was inserted into the mill chuck. In order to do the vertical slot, the table is moved in the y-direction such that it cuts in the same plane as the swivel axis. Three passes were necessary in order to obtain the desired .27" gap. Once this gap was complete, the forth axis was rotated 55° ccw while the end mill was kept at the correct depth in the y-direction. An additional three passes were necessary to complete the desired horizontal gap size. Once completed, the forth axis was rotated back to zero degrees and the table was moved so that the end mill was no longer touching the part. The forth axis was then rotated 180° and the same steps were done to make the same slots on the opposite side. Once complete, the end mill was replaced with a 1/8" drill in order to make the press fit holes on the side. The manufactured swivel nub top can be seen in **Figure 24**.

Figure 24. Manufactured Swivel Nub Top

The only other issue the team ran into in the manufacturing of the swivel nub was the extensive amount of time needed to machine steel. In order to mitigate thermal expansion problems of

dissimilar metals, the clevis and stress beam were both manufactured out of steel. Even though the cuts necessary were very basic, in order to get a good finish, each pass on the lathe was taken very slowly, and only a small amount of material was removed. The tools supplied to us at the Cal Poly machine shop made cutting this harder metal a lot more difficult and resulted in an even longer manufacturing time. The final assembly of the swivel nub can be seen in **Figure 25**.

Figure 25. Manufactured Swivel Assembly

6.2 Casted Swivel Nub

Due to the time intensive manufacturing process of the swivel top, the team looked into casting several of the components through the manufacturing engineering department at Cal Poly for free. A curved slot was inserted into the swivel top in order to aid the rotation of the stress beam as it locked into place. This complex geometry was nearly impossible with the manual machining process, by could be easily made with rapid prototype casting. The team also decided to cast the support bar as one piece to eliminate any thermal expansion problems with the casting material. **Figure 26** below shows the curved slot design of the swivel top and the support bar.

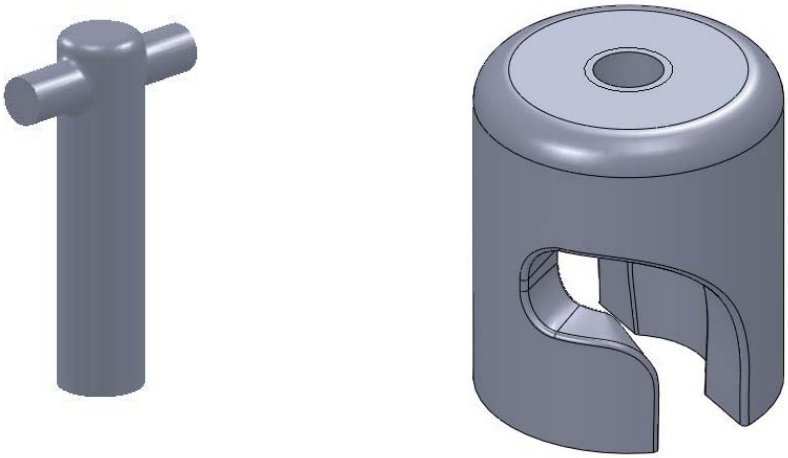

Figure 26. Curved Slot and Cast Support Bar

The material provided by the manufacturing engineering department was ZA-12, a zinc aluminum alloy with a yield strength of 31 ksi. A finite element analysis was conducted on the part with this material and minor dimensional changes were required to ensure the survival of the part. A gating system was also designed into the part to allow the metal to flow into the part. Four or each part were rapid prototyped and put into a pattern. **Figure 27** below shows both patterns ready to be molded.

Figure 27. Swivel and Support Patterns

A plaster mold was made from these patterns and allowed to settle over night. The molds were cured in a furnace and the plastic prototypes were melted out. Once cured, the metal was poured into the mold and allowed to cool. The parts were broken out of the plaster and cut off of the pattern. The finished parts are shown in **Figure 28** below, but the gating system still needs to be removed and the edges need to be ground down.

Figure 28. Casted Swivel Nub

6.3 Socket Stud

The socket stud was the second quick connect design chosen to be manufactured for a final design. The SASM Team chose to manufacture the socket stud at the Cal Poly Machine shop in order to get a quick turnaround time at an inexpensive cost and to gain machining and manufacturing experience.

The Socket Stud and the Safety Collar were the only custom components which needed to be manufactured for this design since all other components are off the shelf. Aluminum was chosen as the manufacturing material due to its easy machining properties. The intricate shape of the socket proved to be difficult to machine, however, over time the procedure became more trivial. There were two separate designs that were manufactured, the first of which can be seen in **Figure 29**. The final socket stud prototype can be seen in Figure 30 and is close to identical to the first prototype except for minor changes to include a stainless steel shoulder bolt at the connecting point. and the design of the complete assembly with the Safety Collar is presented in **Figure 30**.

Figure 29. First Socket Stud prototype

Figure 30. Final Socket Stud prototype

The socket stud manufacturing process started with 1” bar stock in the lathe. The end was faced and the outer diameter was turned down to .75”. Next a .25” through hole was drilled and a .422” hole was drilled to a depth of 1.5”. Care had to be taken on this process since the socket cap screw head sits on this surface. Once the socket was parted and faced the socket hole and slot were milled carefully

using a .25” end mill. The .125 rounds were milled with a smaller bit and then the part was repositioned to drill the shoulder bolt profile. Lastly, the part was deburred and tapped. The safety collar was simple to manufacture and involved turning the outside, drilling a .25” diameter, boring the inside and parting the Safety Collar off.

6.4 Compression Spring Adjustment

The compression spring design was chosen to optimize the suspension mechanism as well as reduce the overall size of the assembly. Three devices were manufactured, all with the same design which can be seen in **Figure 39.** The design before manufacturing went through several iterations to ensure the device would work properly as well as be safe.

The first complete design iteration was changed in order to reduce the outer diameter to 1.3 inches, as well as make it easier to manufacture. The manufacturing process revealed a couple design flaws that made the inner rod unnecessarily difficult to manufacture. In the first iteration, the inner rod had a groove to rotationally fix the inner rod to the housing by means of a key way. That key way was replaced by a slot in the outer housing, which will hold a socket cap screw in place on the inner rod, as seen in **Figure 39.**

Four different process were used to manufacture the final Compression Spring Adjustment Mechanism as seen in **Figure 32.** For the outer housing, the CNC lathe was used to turn the outer dimensions to get a precise diameter as well as a smooth and consistent surface finish. Next, the manual lathe was used to make the internal retaining ring grooves. A special grooving tool was purchased to make this groove. The .25” wide slot was then milled into the side of the Outer Housing. The majority of the inner rod was manufactured on the lathe. The outside diameter was turned to the proper diameter of .5” and then the hole through the center was drilled with specially purchased extended reach drill bits.

Although the manufacturing process is extensive, the benefit of the Compression Spring Adjustment Mechanism over the current spring and turnbuckle system greatly outweighs this fact.

Figure 31. Spring Adjustment Mechanism Exploded View

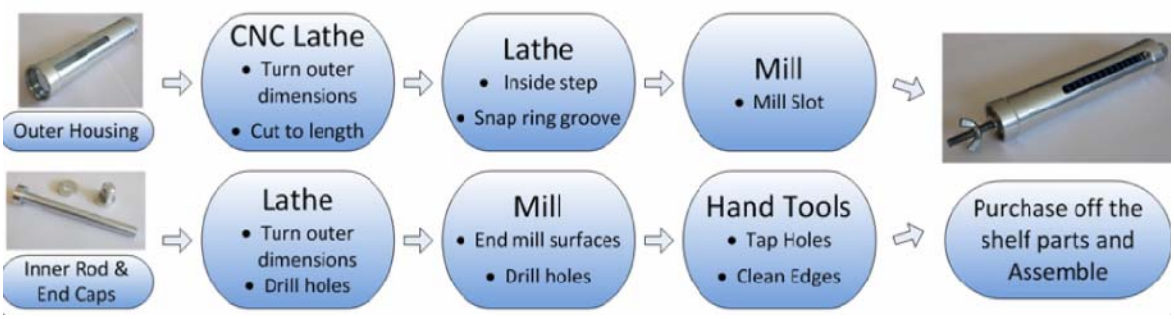

Figure 32. Manufacturing process of the Compression Spring Adjustment Mechanism

7 Design Verification (Testing)

7.1 Approach and Methodology

The first step in verifying the functionality of a design is to highlight all the high risk failure modes. Once the high risk areas are predicted, tests can be completed to verify the severity, occurrence or detection rating of a particular failure mode. Depending on the results, a mitigation plan can be completed to reduce the severity and occurrence, or to increase the detection rate of the failure. A Design Failure Mode and Effects Analysis was completed for the each subsystem including the force gauge, adjustment mechanism, and quick connect. Suspect high risk failures can be seen in **Appendix M**.

For each sub-system, failure modes were established and were rated by severity, occurrence and detection rating. The severity ratings ranged from 10, meaning the failure has the potential to permanently damage the customer or the panels, all the way down to 1, meaning that the failure would not even be noticeable and would have no affect on the customer or the panels. The occurrence rating ranged from 10, meaning failure is almost inevitable, to 1, meaning the failure is extremely unlikely. The last set of predictions deals with the current controls of how to mitigate the failure. All of the preventative actions which can be made by the user or the team were outlined, along with any detection mechanisms built into the design. With both of these measurements accounted for, the detection rating was predicted, and they ranged from 1, meaning that the defect is obvious and will certainly be detected, to 10, meaning the device is not able to be inspected for the particular failure mode. In order to quantify the risk of each failure mode, the severity, occurrence and detection ratings were multiplied together to yield a level of risk. We only considered making tests for levels of risk above 100 and a list of these tests can be seen in **Appendix N**.

7.2 Test Descriptions and Results

The first test is the unthreading test. This test is meant to measure how much the adjustment mechanism unthreads due to a 300 pound load. This test was done by loading the adjustment in tension in the Instron machine and watching to see if the outer housing rotated due to the applied load. The test showed that the adjustment did not unthread during the loading and all expansion was due to the strain placed upon the system.

The second test is the Thermal cooling test, and was completed on the swivel nub, socket stud and adjustment mechanism. This test proves that the system can go through a full cooling cycle without sustaining any major damage. The parts were cooled in a sealed foam container with dry ice while being monitored by thermo, and can be seen in **Figure 33**. It took approximately 20 minutes for the parts to reach thermal equilibrium of about -70°C within the foam container. The parts were then taken out and allowed to warm back up to room temperature. After the parts had warmed back up they were inspected. This was conducted by visual inspection of the parts using a magnifying glass. No cracks or signs of wear were discovered on the parts that had been cooled and reheated.

The third test was to check if the severe temperature drop would cause the parts to seize and was done in conjunction with the second test. After all the parts were cooled and reheated from the second test, the team verified that all of the parts were able to either disconnect or adjust properly.

Figure 33. Cooling of the Socket Stud

The fourth and fifth tests were conducted by putting the swivel nub, socket stud and adjustment mechanism in tension to 300 pounds. The tensile machine was set to stretch the quick connects at a rate of .01 in/min in order to test the quasi-static properties. The tests looked to see if the components

experienced yielding or surpassed their ultimate strength for an applied load of 300lbs. The test was conducted in the Instron machine while the parts were at room temperature and then the parts were cooled to -70°C in the foam test chamber loaded to 300 pounds again. The test set up for both the cryogenic and room temperature tensile testing can be seen in **Figure 34** and **Figure 35**. The internal temperature was monitored with thermocouples and a summary of test data can be found in Table 6. None of the parts failed during loading or showed signs of yielding.

Figure 34. Room Temperature Tensile Testing

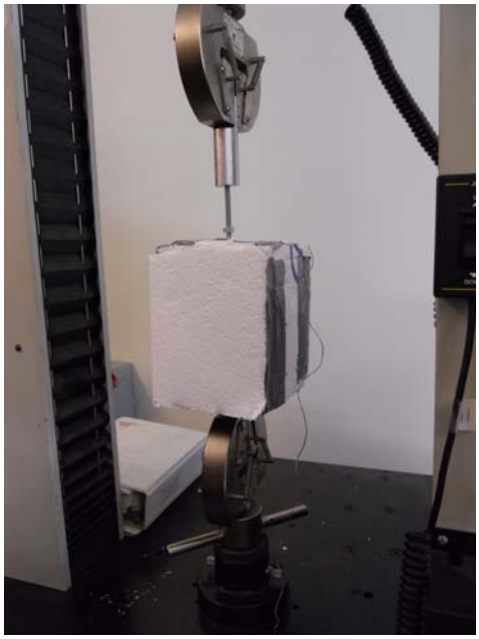

Figure 35. Cryogenic Tensile Testing

Table 6. Room Temperature and Cryogenic Test Data

	Room Temperature		Cryogenic Test			
Part	Max Load [lbs]	Delta L [in]	Max Load [lbs]	Delta L [in]	Initial Temp [Celsius]	Final Temp [Celsius]
Swivel Nub	300	0.031	300	0.039	-68.3	-62.4
Extension Mechanism	Note A	3	390	2.663	-69.8	-60
Socket Stud	300	0.048	311	0.041	-68.7	-70.6
Cast Swivel Nub	300	0.022	305	0.015	-66	Note B
Cast S. N. to Failure	1038	0.51				

Note A: machine Pulled to a force greater then 1000 lbs

Note B: Thermo Couple Broke and no more data could be taken

The previous five tests proved the functionality of both the quick connect designs and the adjustment mechanism, but did not test the ergonomics. This was done in tests 6 and 7, and was used to make the final decision on which quick connect device to use in the final assembly. Both the socket stud and swivel nub were placed in series with the adjustment mechanism, and the team members took turns connecting and disconnecting the mechanisms. Data was taken on how much time it took to make the connections and adjustments to a load of 30 pounds. It was found that both connectors were able to connect within two seconds, which is well below the accepted value of 10 seconds. The adjustment time was found to be less than 10 seconds, which is well below the accepted value of 30 seconds. Since both quick connect designs tested similarly across the field, the design with the least amount of components and the easiest manufacturing was chosen to be in the final design, which is the Socket Stud.

In order to verify that the socket stud was definitely operated in the elastic region, strain gauges were attached to it and stress and strain values were recorded up to a load of 2400 pounds. As seen in **Figure 36** the stress-strain correlation is linear up to a stress of about 10,000 psi. This confirms that the socket stud will not plastically yield at 300 pounds, which correlates to a stress of 1345 psi. One concern about this analysis is that the experimental elastic modulus of 40 million Psi is about four times higher than the theoretically accepted value of 10 million Psi. One explanation for this difference is that the strain gauges were placed very close to the edge of the slot and could have been picking up strain in a stress concentrated area, as seen in **Figure 37**. In addition, due to the geometry of the Socket Stud, the location picked for the strain gauges was also in bending, which would increase the elastic modulus.

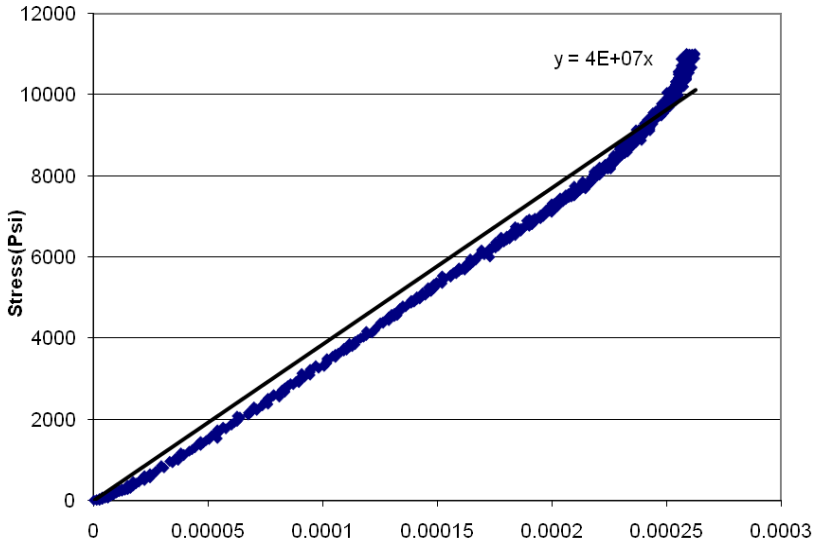

Figure 36. Socket Stud Stress vs. Strain Graph

Figure 37. Strain Testing on Socket Stud

8 Final Design

8.1 Assembly Description

The final assembly shown in **Figure 38** consists of the current analogue force gauge, the current large adjustment bar, a compressed spring adjustment, and the socket stud quick connect. It provides a quick way for technicians to reliably connect and disconnect solar panel arrays for testing without the use of tools or loose parts. The analogue force gauge was chosen due to its ease of use, availability and reliability in both the thermal testing environment and standard clean room. Both alternative solutions failed to improve the existing design, and the load cell concept in particular would've added risk and complications to the overall system by introducing electrical components into an untested environment. Two shackles in series will attach the analogue force gauge to the large adjustment bar. Another shackle will be used to connect the large adjustment bar to the compressed spring adjustment mechanism. The compressed spring adjustment was chosen because it combines the minor adjustments along with the compression spring into one sub-assembly. It provides a reliable solution for both the standard and cryogenic testing rooms and utilizes basic components which were relatively easy to manufacture. The adjustment mechanism will be connected to the socket stud by a bearing swivel eye clevis. Even though the socket stud and swivel nub tested similarly, the socket's stud ease of manufacturing and reduced number of components made it the more appealing solution. A complete detailed drawing of the assembly can be seen in **Appendix C**.

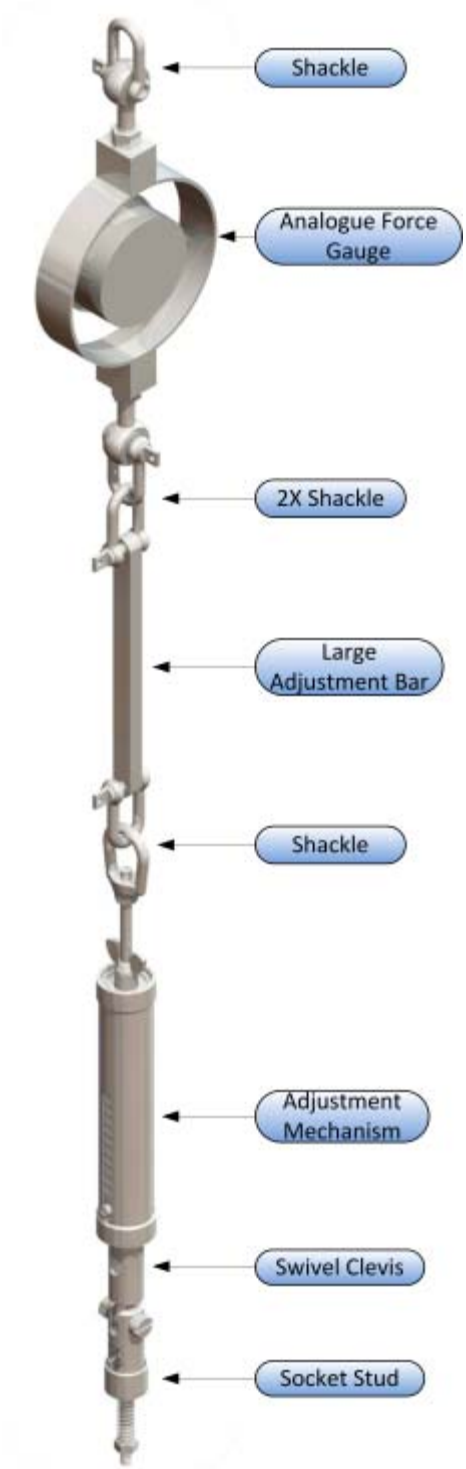

Figure 38. SASM Final Assembly

A summary of the specifications and if they were met by the final design can be seen in **Table 7**. The final design met all of the requirements except for being able to connect under a load. The adjustment

mechanism will need to be used to displace the Socket Stud low enough to engage the socket cap screw. Once connected, the adjustment can be raised to displace the correct load.

Table 7. Final Specification Table

Overall System Specifications				
Spec #	Parameter Description	Requirement or Target (units)	Tolerance	Verified
1	Number of Tools Required	0	Max	Yes
2	Quantity of Loose parts	0	Max	Yes
3	# of Actions Required to Operate	3 actions	Max	Yes
4	Visibility of Parts	All (High)	N/A	Yes
5	Width Dimensions	1.3 Inches	Max	Yes
6	Load Allowable	100 lb	+200lb	Yes
7	Cost	$8,000	Max	Yes: $2,900
8	Weight	8 lb	Max	Yes
9	Temperature Range	-80 C to 50 C	Range	Yes
10	Clean Room Compatible	0 Intrusive Elements	Max	Yes

Specific Adjustment Mechanism Specifications				
Spec #	Parameter Description	Requirement or Target (units)	Tolerance	Verified
13	Operation Time of Adjustments	30 Seconds	Max	Yes: <10 seconds
14	Pitch Resolution	1/14"	+/-1/28	Yes

Specific Quick Connect Specifications				
Spec #	Parameter Description	Requirement or Target (units)	Tolerance	Verified
15	Operation Time for Connecting	5 seconds	Max	Yes: Under 2 seconds
16	Unload / Loading Deflection	3/4 inch	+/- 1/4"	No: Adjustment required for connection

8.2 Adjustment / Spring Mechanism Description

The compression spring adjustment mechanism provides a reliable and quick method to accurately redistribute force among the different SASMs and is seen in **Figure 39**. It was the highest ranking concept in the decision matrix, and passed all the strength and slip tests without fault. The combination of the spring and adjustment mechanism is so great because it decreases the overall height to make it compatible with the shorter thermal testing chamber. It also eliminates the need to install extra safety components during proof testing.

Figure 40. Compression Spring Section View

The compression spring adjustment attaches near the bottom of the assembly right above the ball bearing swivel and the connection mechanism. The bottom cap is capable of connecting directly to the ball bearing swivel, reducing the need for extra components. The purpose of the bottom cap is to keep the inner rod from displacing axially and is held in the outer housing by a stainless steel retaining ring, which has a 225 Ksi tensile stress rating. Retaining rings were used instead of screws to hold the top and bottom caps in place instead of screws in order to reduce the overall diameter, piece parts, and stress concentrations. The inner rod is adjacent to the bottom cap and travels through the center of the spring and exits on the other end of the outer housing, as seen in the section view of **Figure 40**. It holds a dual purpose of holding the compression spring in place while allowing the threaded rod to thread into it. The spring is confined vertically by the inner rod flange and the top plate. It is confined radially by the outer housing and the inner rod. This keeps the spring from buckling under max loads, and tests have shown no adverse effects during proof loading to 300 pounds. A socket cap screw is inserted into the flange of the inner rod in order to rotationally fix it to the outer housing. This way,

Figure 39. Spring Adjustment Mechanism Exploded View

when the outer housing is spun, the inner rod rotates with it, allowing the threaded rod to thread into or out of the inner rod. This movement will be simple for an operator to perform since he or she does not have to loosen two sides of a turnbuckle before adjusting the height. Since mechanical failure in any section of the SASM is unacceptable, adjustment mechanism was designed robustly and drawings can be seen in **Appendix D**.

8.3 Socket Stud Description

The Socket Stud provides a secure connection between the SASM and the solar arrays. It is simple to operate, easy to manufacture, and requires no tools to operate. The design includes only two manufactured components, the socket stud and the safety, and five off the shelf parts. The complete assembly can be seen in **Figure 41** and a detailed drawing can be found in **Appendix E.** The socket cap screw replaces the current clevis, and is threaded into the solar array's ¼-28 embedded hole while the socket stud is attached to the bottom end of the SASM. In order to connect the socket stud to the socket cap screw, the operator pulls down on the socket stud and displaces the safety. The slot in the socket stud is aligned with the head of the socket cap screw and is slid under the head of the screw to connect. The operator pulls down on the socket to align the socket opening with the head of the screw and slides it in. The screw head is kept from easily sliding out by sitting in a .1 inch deep groove. Once the bolt is in place, the safety collar displaces upward due to the spring activation and it encompasses the opening in the socket stud in order to assure no accidental disconnects.

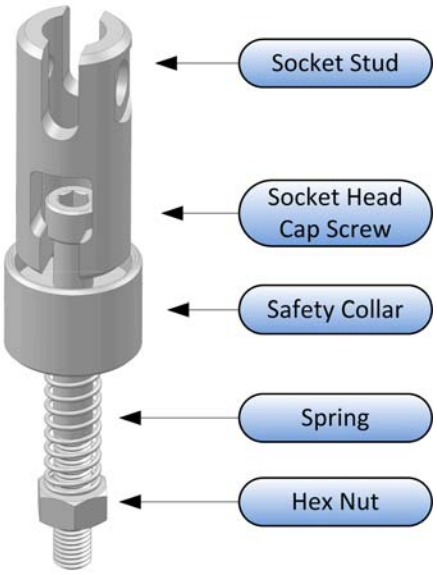

Figure 41. Socket Stud Assembly

8.4 Future Build Considerations

Future builds of the SASM should be made out of steel instead of aluminum. Even though the manufactured aluminum parts passed all of the strength requirements, they were easily marred during tests and showed signs of wear after only a few cycles. Also, by making everything out of steel, it would make the assembly expand and contract homogenously. In addition, it is important to note that any socket head cap screw length can be used in order to incorporate the depth of the alignment cube used to keep the solar arrays locked when not being deployed.

8.5 Analysis Results

As outlined earlier, the main operation of the Solar Array Suspension Mechanism is to support the weight of solar panels in a quasi-static environment. The typical load seen by the Suspension Mechanism is around 100lb. A factor of safety of 3 was introduced to the load in order to account for an unexpected increase or misuse of the device. This load of 300lbs was then used for all analysis and factors of safety are derived for this load.

Initial analysis was done using classical mechanics of materials. Using the typical published yield strengths for Aluminum in *Shigliey's Mechanical Engineering Design 8th Edition,* geometric properties like wall thicknesses and part sizes were derived. These induced stresses were based on the 300lb load criteria. Hand calculations were completed on all of the quick connect concepts including the Carabiner, Pneumatic, Swivel Nub, Socket Stud and U-Loop and can be seen in Appendix F through Appendix K. Using these methods the original size of the components was determined and used to generate the initial solid models.

In order to verify these initial designs Finite Element Analysis was used on the models chosen to be manufactured, including the Swivel Nub and Socket Stud. The FEA was done using linear static elements. Each component was imported from solid works individually and analyzed using ABAQUS. Each component of each sub assembly was pinned at the locations where is would be in contact with the component located above it. For the components that interfaced with threads the embed criteria was used as a boundary condition for the surface area that would be in contact with the threads. The load was always applied to the lowest area of contact as a resulting pressure.

To gauge the accuracy of the FEA a mesh convergence for a critical point was preformed. The mesh convergence was done by relating the stress at that particular node to the number of degrees of freedom used in the analysis. When the stress did not change by a significant amount (ie 5%) that size element and mesh was used for the analysis of the whole part. The mesh convergence and FEA models can be found for the Swivel Nub in **Appendix I** and the Socket Stud in **Appendix J**. The node with the maximum stress was then compared to the yield strength of the material that was used to machine it. The factor of safety for each part is defined as the maximum stress from the FEA divided by the yield strength for that material. A simple force over area stress calculation was completed for the outer housing of the adjustment mechanism at the thinnest area where the retaining ring sits. An FEA model was quickly completed to verify these simple hand calculations, and the results correlated nicely. A summary of these FOS can be found in **Table 8**.

Table 8. Factor of Safety for Each Component

	Maximum Stress (Kpsi)	Yield Strength (Kpsi)	FOS for 300lb Load
Swivel Nub	33.2	42 (Aluminum)	1.27
Socket Stud	8		5.2
Adjustment	1.3		30

In order to check the accuracy of the FEA analysis a model of the Cast Swivel Nub was used to predict a failure region and failure mode at ultimate strength. The Cast Swivel Nub was brought to failure and then compared to the FEA analysis in order to verify the model. **Figure 42** shows the point of failure of the Cast Swivel Nub.

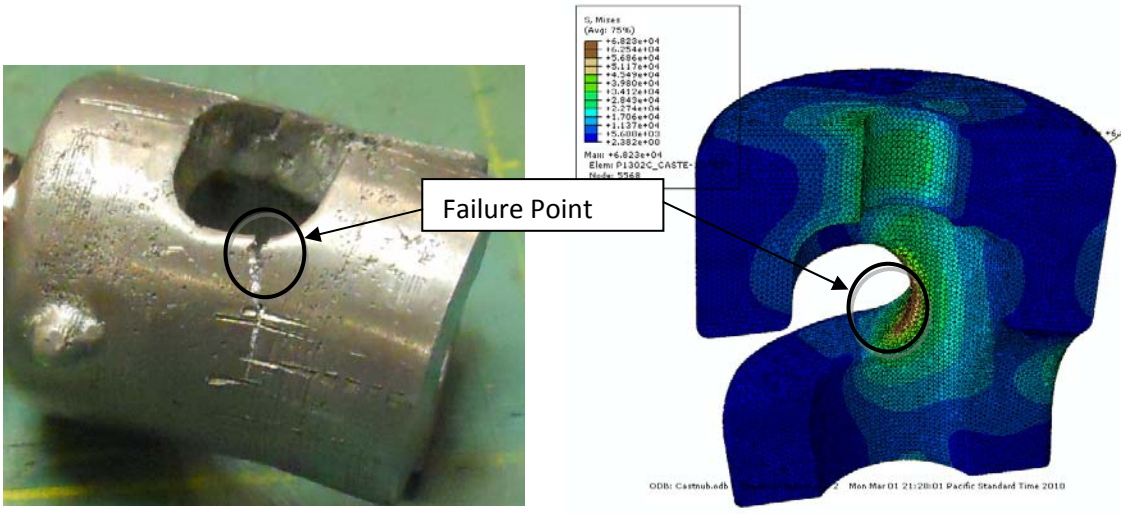

Figure 42. Failure Point Compared to FEA

In addition to doing a Finite Element Analysis, the team also completed a Coefficient of Thermal Expansion analysis on the final assembly. The goal was to quantify the maximum deflection due to thermal strain of the Adjustment Mechanism and Socket Stud when placed in series. In order to simplify the calculations, and to have the analysis valid for future builds, the material used in the analysis was steel. Steel has a coefficient of thermal expansion of $9.6\frac{\mu in}{in \bullet °F}$. The temperature range used in the calculations was from 25°C to -80°C. The complete analysis can be seen in **Appendix L**, and the results showed a change in length of merely -.032 inches. If it can be assumed that all of the Solar Array Suspension Mechanisms are in parallel, and are of the same material, then they should all uniformly contract. This means that no stress concentrations due to thermal contraction should form at the hinges of the solar arrays.

8.6 Cost Breakdown

Each SASM assembly as defined by the design specifications had a maximum cost of $8000. The SASM team successfully designed a robust and reliable system for significantly less with an approximate total of $2900 as shown in **Table 9**. This cost is based on our final design which includes the current analogue ring force gauge, current square bar long adjustment, Compression Spring Adjustment Mechanism, and Socket Stud quick connect. The exact cost of the analogue ring force gauge was unknown to the team so it was estimated to be $1500. The cost of the machined components are highlighted in blue on **Table 9** and was estimated based on the time it took the SASM Team to machine each component and the hourly rates of a local machine shop, Snider Precision, plus the cost of material. It should be noted that the cost of manufacturing these devices will vary depending on the manufacturer as well as the number of devices to be made.

Table 9. Cost estimate for one SASM device

Sub Assembly	Component	SASM Machine Time [Hours]	Estimated Cost [$]
Force Gauge	Analogue Ring Gauge	-	1500
Long Adjustment	Square Bar	-	50
Compression Spring Adjustment Mechanism	Outer housing	1.5	135
	Inner rod	1.5	135
	Top cap	.25	25
	Bottom cap	.75	75
	2 X Internal retaining ring	-	4
	Chrome-silicon steel die spring	-	8
	Socket cap screw	-	1
	Threaded rod	.25	30
	Hex nut	-	1
	SS oval eye nut	-	16
	SS E-style retaining ring	-	1
	Wing nut	-	2
Compression Spring Adjustment Mechanism Total:		4.0	370
Socket Stud	Socket Stud	2	165
	Safety Collar	.5	50
	Socket Cap Screw	-	1
	Hex Nut ¼-28	-	1
	Steel Compression Spring	-	1
	Shoulder Screw	-	3
	Hex Nut ¼-20	-	1
Socket Stud Total:		2.5	215
Miscellaneous	Ball Bearing Swivel	-	70
	4 X D-Shackle	-	40
Total Cost:			2900

The SASM team was budgeted by ATK $2,500 to complete this design challenge. The team was well under the designated budget and spent approximately $740 for raw material, off the shelf parts, tooling, and testing and display fixtures. The expenditure breakdown can be seen in **Appendix O** and includes prices of raw material, hardware and an estimate of shipping and fixture costs.

9 Conclusion

The final design presented by the Solar Suspension Technologies team surpassed the design requirements presented by ATK. The proposed SASM has no removable parts, requires no tools to operate and can easily adjust its length. This final assembly includes the analog force gage that is currently used by ATK, a compression spring adjustment mechanism, bars for long adjustments and a Socket Stud quick connection device. The mechanism will also operate in the required cryogenic temperatures without part fatigue or failure. The estimated total cost for the proposed SASM is $2900, which is significantly less than the specified total cost of $8000. The team is satisfied with the results of the design and look forward to the implementation of the SASM at ATK Space.

Index to Appendices

Appendix A: Quality Function Deployment

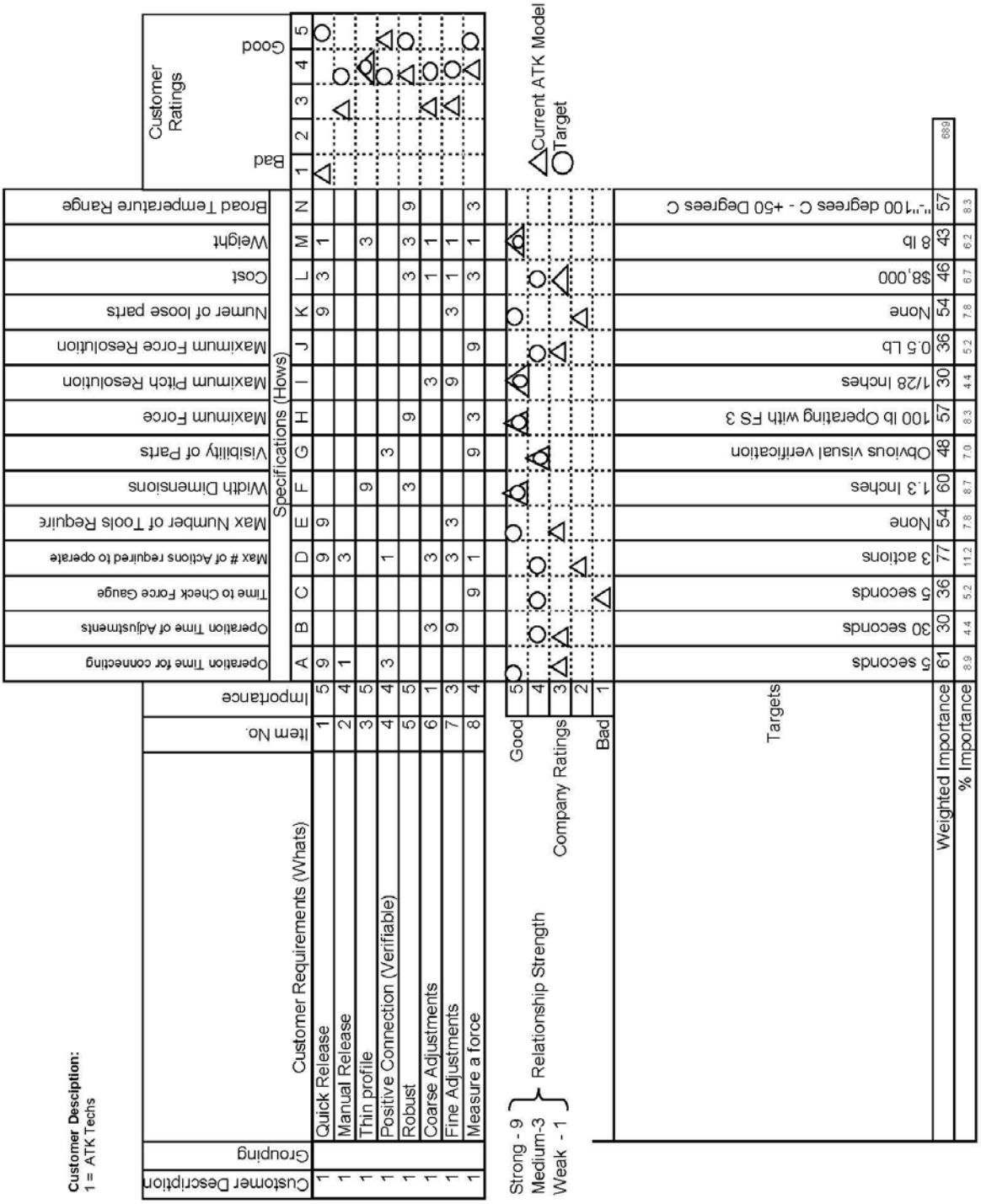

Appendix B: Gantt Chart

ID	Task Name	Duration	Start	Finish
1	**Project Proposal**	**8 days**	**Tue 10/6/09**	**Thu 10/15/09**
2	QFD Analysis	4 days	Thu 10/8/09	Tue 10/13/09
3	Prepare Shedule and Gantt Chart	6 days	Thu 10/8/09	Thu 10/15/09
4	Background Research	8 days	Tue 10/6/09	Thu 10/15/09
5	Detailed Schedule	5 days	Fri 10/16/09	Thu 10/22/09
6	Gantt Chart	5 days	Fri 10/16/09	Thu 10/22/09
7	**Concept Design Review**	**17 days**	**Tue 10/13/09**	**Tue 11/3/09**
8	**Idea Generation**	**5 days**	**Tue 10/13/09**	**Mon 10/19/09**
9	Brainstorm Chart	3 days	Tue 10/13/09	Thu 10/15/09
10	Subcategory mapping	2 days	Fri 10/16/09	Mon 10/19/09
11	Sketches of Designs	2 days	Tue 10/20/09	Wed 10/21/09
12	Decision Matrix	2 days	Thu 10/22/09	Fri 10/23/09
13	Compile Presentation	3 days	Sun 10/25/09	Tue 10/27/09
14	Create Design Report	7 days	Mon 10/26/09	Tue 11/3/09
15	Design Verification Plan	7 days	Wed 11/4/09	Thu 11/12/09
16	Critical Design Review	51 days	Fri 11/13/09	Fri 1/22/10
17	CAD Modeling and Drawings	36 days	Fri 11/13/09	Fri 1/1/10
18	Final Design Report	15 days	Mon 1/4/10	Fri 1/22/10
19	**Draft Design Status Report**	**9 days**	**Mon 1/25/10**	**Thu 2/4/10**
20	Finalize Drawings	5 days	Mon 1/25/10	Fri 1/29/10
21	BOM Development	5 days	Mon 1/25/10	Fri 1/29/10
22	Compile Report	9 days	Mon 1/25/10	Thu 2/4/10
23	**Build Full Assembly**	**35 days**	**Mon 1/25/10**	**Fri 3/12/10**
24	**Build Connection Mechanism**	**33 days**	**Mon 1/25/10**	**Wed 3/10/10**
25	Order Raw Materials	14 days	Mon 1/25/10	Thu 2/11/10
26	Manufature Components	21 days	Mon 2/1/10	Mon 3/1/10
27	Assemble Mechanism	7 days	Tue 3/2/10	Wed 3/10/10
28	**Build Adjustment Mechanism**	**35 days**	**Mon 1/25/10**	**Fri 3/12/10**
29	Order Raw Materials	14 days	Mon 1/25/10	Thu 2/11/10
30	Manufacture Components	14 days	Fri 2/12/10	Wed 3/3/10
31	Assemble Mechanism	7 days	Thu 3/4/10	Fri 3/12/10
32	Prototype and Test Plan Review	3 days	Mon 3/15/10	Wed 3/17/10
33	**Hardware Test**	**40 days?**	**Mon 1/25/10**	**Fri 3/19/10**
34	**Build Test Fixture**	**34 days?**	**Mon 1/25/10**	**Thu 3/11/10**
35	Design Stregth Test Fixture	9 days?	Tue 2/9/10	Fri 2/19/10
36	Purchase Fixture Components	9 days?	Mon 2/22/10	Thu 3/4/10
37	Setup Cryo testing with Materials Lab	7 days	Mon 1/25/10	Tue 2/2/10
38	Design Cryogenic Component	14 days?	Mon 2/22/10	Thu 3/11/10
39	Conduct Yield Testing	10 days	Mon 3/8/10	Fri 3/19/10
40	Final Hardware Demo	41 days?	Mon 3/15/10	Mon 5/10/10
41	Final Project Report	45 days?	Mon 4/5/10	Fri 6/4/10

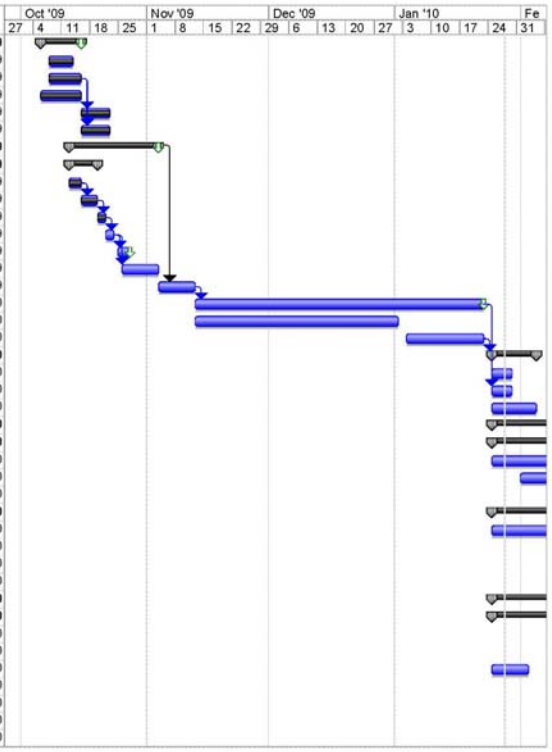

:

ID	Task Name	Duration	Start	Finish
1	**Project Proposal**	**8 days**	**Tue 10/6/09**	**Thu 10/15/09**
2	QFD Analysis	4 days	Thu 10/8/09	Tue 10/13/09
3	Prepare Shedule and Gantt Chart	6 days	Thu 10/8/09	Thu 10/15/09
4	Background Research	8 days	Tue 10/6/09	Thu 10/15/09
5	Detailed Schedule	5 days	Fri 10/16/09	Thu 10/22/09
6	Gantt Chart	5 days	Fri 10/16/09	Thu 10/22/09
7	**Concept Design Review**	**17 days**	**Tue 10/13/09**	**Tue 11/3/09**
8	**Idea Generation**	**5 days**	**Tue 10/13/09**	**Mon 10/19/09**
9	Brainstorm Chart	3 days	Tue 10/13/09	Thu 10/15/09
10	Subcategory mapping	2 days	Fri 10/16/09	Mon 10/19/09
11	Sketches of Designs	2 days	Tue 10/20/09	Wed 10/21/09
12	Decision Matrix	2 days	Thu 10/22/09	Fri 10/23/09
13	Compile Presentation	3 days	Sun 10/25/09	Tue 10/27/09
14	Create Design Report	7 days	Mon 10/26/09	Tue 11/3/09
15	Design Verification Plan	7 days	Wed 11/4/09	Thu 11/12/09
16	Critical Design Review	51 days	Fri 11/13/09	Fri 1/22/10
17	CAD Modeling and Drawings	36 days	Fri 11/13/09	Fri 1/1/10
18	Final Design Report	15 days	Mon 1/4/10	Fri 1/22/10
19	**Draft Design Status Report**	**9 days**	**Mon 1/25/10**	**Thu 2/4/10**
20	Finalize Drawings	5 days	Mon 1/25/10	Fri 1/29/10
21	BOM Development	5 days	Mon 1/25/10	Fri 1/29/10
22	Compile Report	9 days	Mon 1/25/10	Thu 2/4/10
23	**Build Full Assembly**	**35 days**	**Mon 1/25/10**	**Fri 3/12/10**
24	**Build Connection Mechanism**	**33 days**	**Mon 1/25/10**	**Wed 3/10/10**
25	Order Raw Materials	14 days	Mon 1/25/10	Thu 2/11/10
26	Manufature Components	21 days	Mon 2/1/10	Mon 3/1/10
27	Assemble Mechanism	7 days	Tue 3/2/10	Wed 3/10/10
28	**Build Adjustment Mechanism**	**35 days**	**Mon 1/25/10**	**Fri 3/12/10**
29	Order Raw Materials	14 days	Mon 1/25/10	Thu 2/11/10
30	Manufacture Components	14 days	Fri 2/12/10	Wed 3/3/10
31	Assemble Mechanism	7 days	Thu 3/4/10	Fri 3/12/10
32	Prototype and Test Plan Review	3 days	Mon 3/15/10	Wed 3/17/10
33	**Hardware Test**	**40 days?**	**Mon 1/25/10**	**Fri 3/19/10**
34	**Build Test Fixture**	**34 days?**	**Mon 1/25/10**	**Thu 3/11/10**
35	Design Stregth Test Fixture	9 days?	Tue 2/9/10	Fri 2/19/10
36	Purchase Fixture Components	9 days?	Mon 2/22/10	Thu 3/4/10
37	Setup Cryo testing with Materials Lab	7 days	Mon 1/25/10	Tue 2/2/10
38	Design Cryogenic Component	14 days?	Mon 2/22/10	Thu 3/11/10
39	Conduct Yield Testing	10 days	Mon 3/8/10	Fri 3/19/10
40	Final Hardware Demo	41 days?	Mon 3/15/10	Mon 5/10/10
41	Final Project Report	45 days?	Mon 4/5/10	Fri 6/4/10

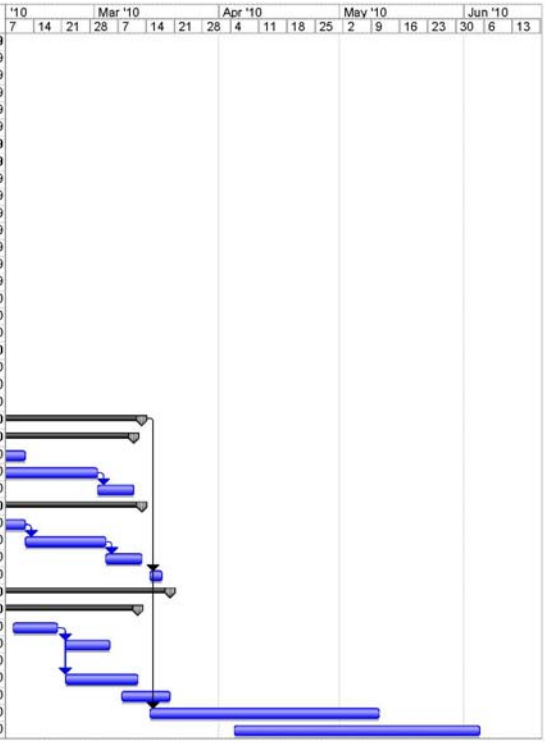

Appendix C: SASM Final Assembly Drawing

ITEM NO.	PART NUMBER	DESCRIPTION	QTY.
1	8928T13	Bearing Swivel	1
2	2168ct1301-1	Adjustment Bar	1
3	3841T53	D-Shackle W/ Self-Locking Screw Pin, 1/4" Dia, 1212# WII	4
4	1100	Analog Force Gauge	1
5	1200	Compression Spring Adjustment Mechanism	1
6	1300D	Socket Stud	1

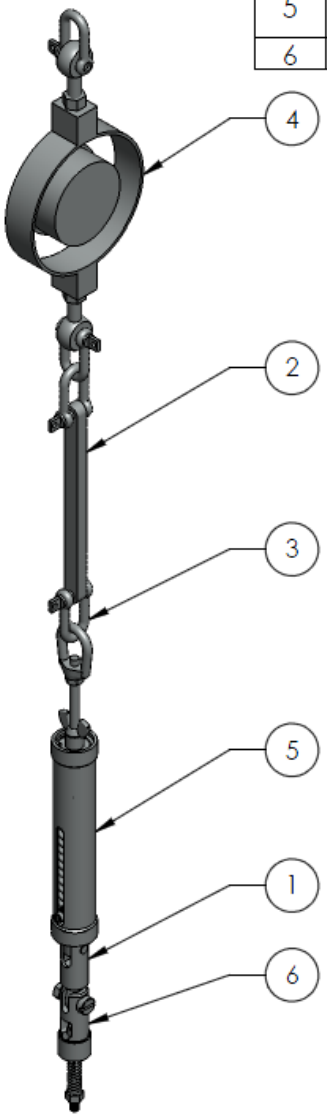

Mechanical Engineering CAL POLY

DRAWN BY: Alex Gould	DATE: 6/02/2010
Master Assembly	
SIZE: A	DWG. NO.: 1000
SCALE: 1:4	WEIGHT:
SHEET 1 OF 1	

Appendix D: Compression Spring Adjustment Drawing

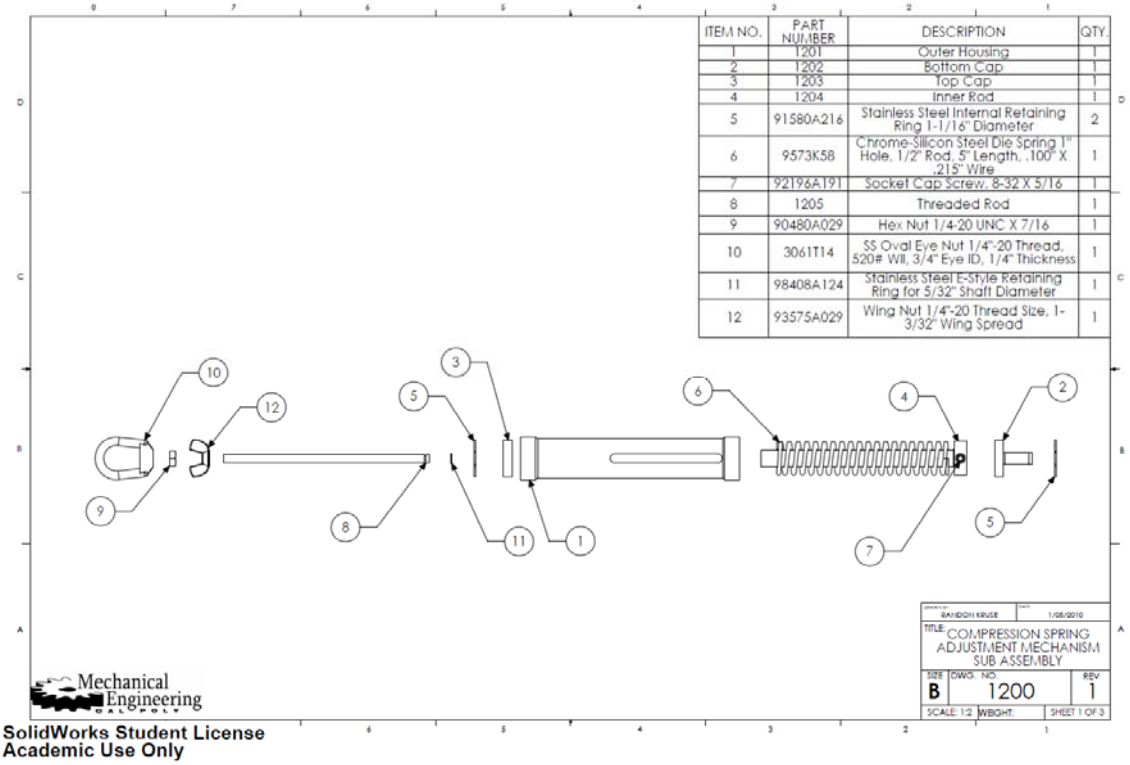

ITEM NO.	PART NUMBER	DESCRIPTION	QTY.
1	1201	Outer Housing	1
2	1202	Bottom Cap	1
3	1203	Top Cap	1
4	1204	Inner Rod	1
5	91580A216	Stainless Steel Internal Retaining Ring 1-1/16" Diameter	2
6	9573K58	Chrome-Silicon Steel Die Spring 1" Hole, 1/2" Rod, 5" Length, .100" X .215" Wire	1
7	92196A191	Socket Cap Screw, 8-32 X 5/16	1
8	1205	Threaded Rod	1
9	90480A029	Hex Nut 1/4-20 UNC X 7/16	1
10	3061T14	SS Oval Eye Nut 1/4"-20 Thread, 520# Will, 3/4" Eye ID, 1/4" Thickness	1
11	98408A124	Stainless Steel E-Style Retaining Ring for 5/32" Shaft Diameter	1
12	93575A029	Wing Nut 1/4"-20 Thread Size, 1-3/32" Wing Spread	1

RANDON KRUSE 1/08/2010
TITLE: COMPRESSION SPRING ADJUSTMENT MECHANISM SUB ASSEMBLY
SIZE B | DWG. NO. 1200 | REV 1
SCALE: 1:2 | WEIGHT: | SHEET 1 OF 3

Mechanical Engineering CAL POLY

SolidWorks Student License
Academic Use Only

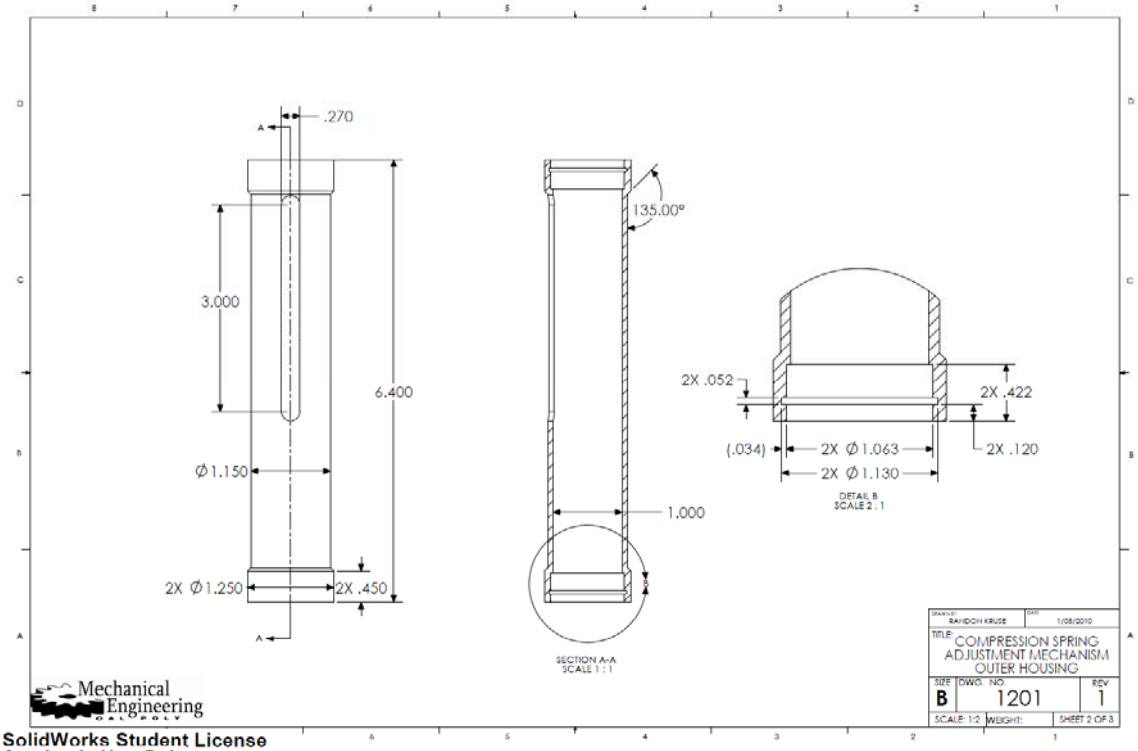

RANDON KRUSE 1/08/2010
TITLE: COMPRESSION SPRING ADJUSTMENT MECHANISM OUTER HOUSING
SIZE B | DWG. NO. 1201 | REV 1
SCALE: 1:2 | WEIGHT: | SHEET 2 OF 3

Mechanical Engineering CAL POLY

SolidWorks Student License
Academic Use Only

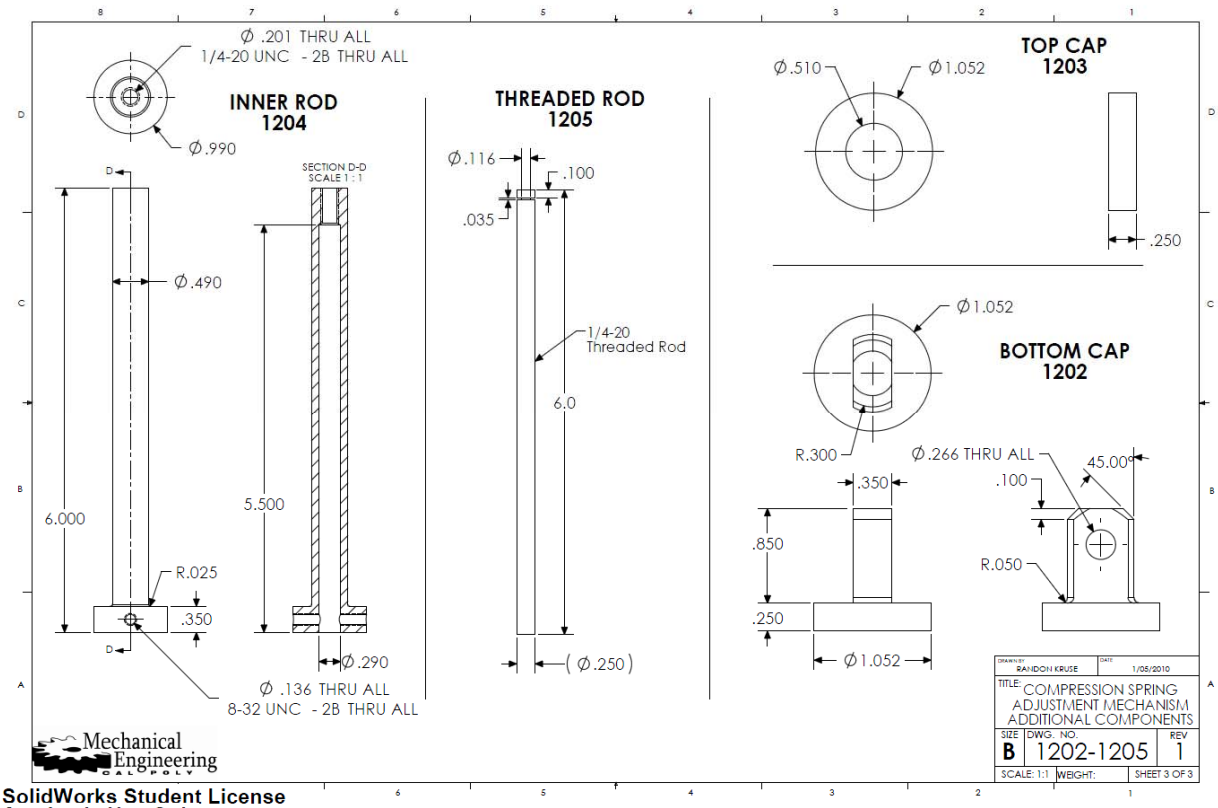

SolidWorks Student License
Academic Use Only

Appendix E: Socket Stud Assembly Drawing

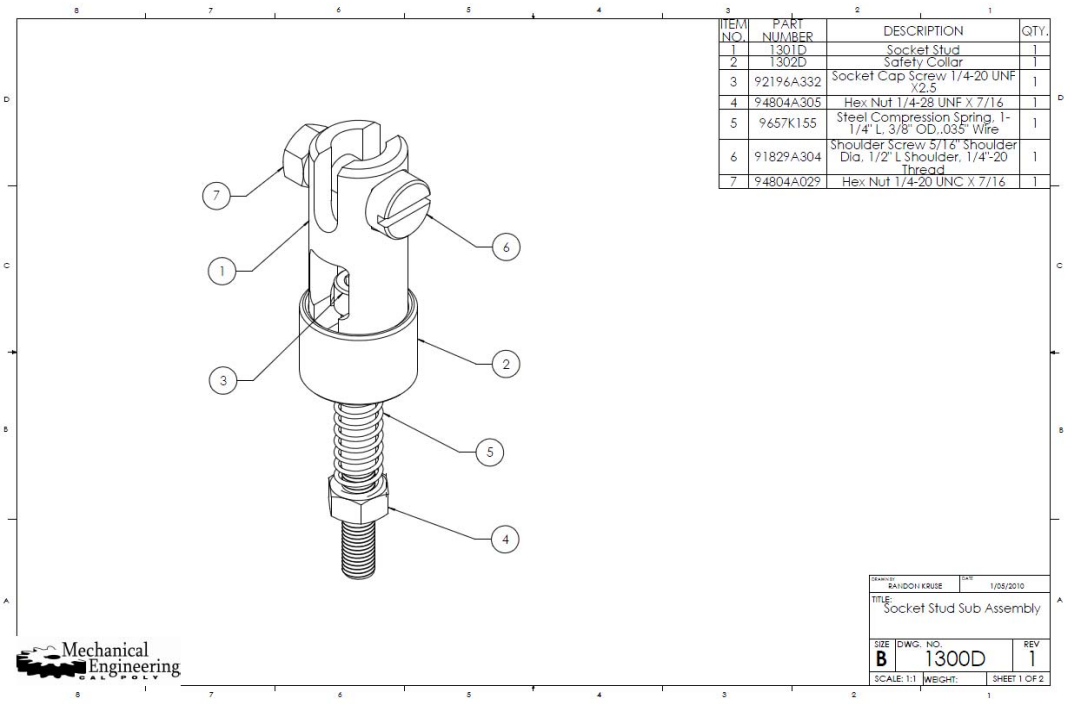

SolidWorks Student License
Academic Use Only

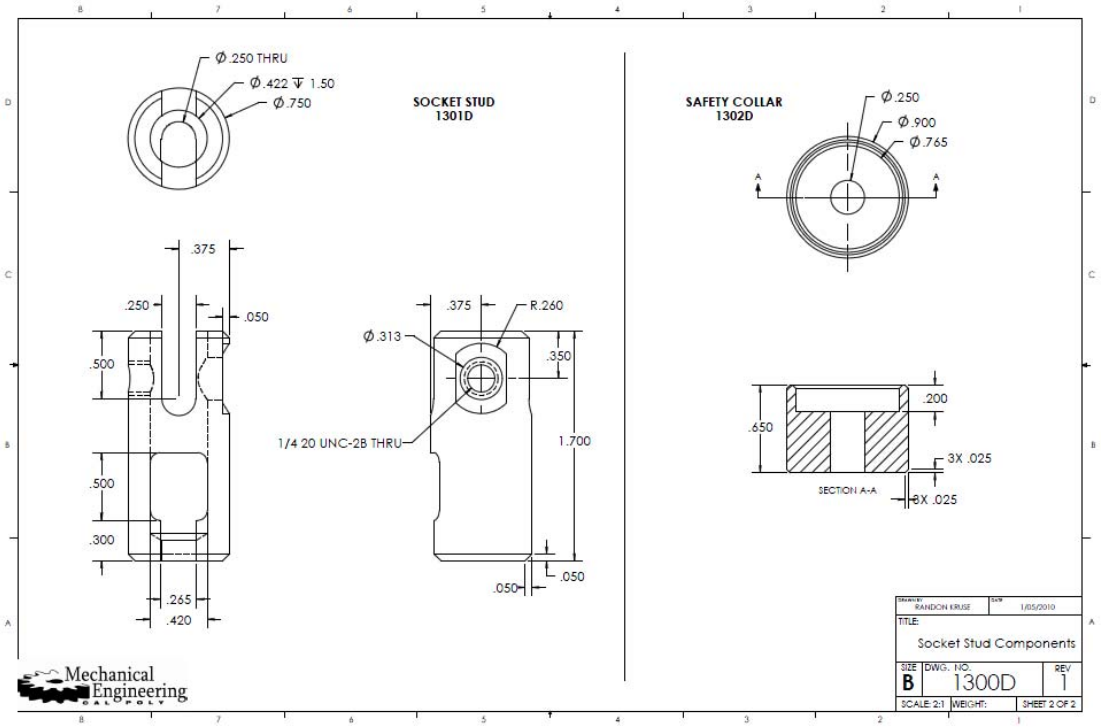

SolidWorks Student License
Academic Use Only

Appendix F: Swivel Nub Assembly Drawing

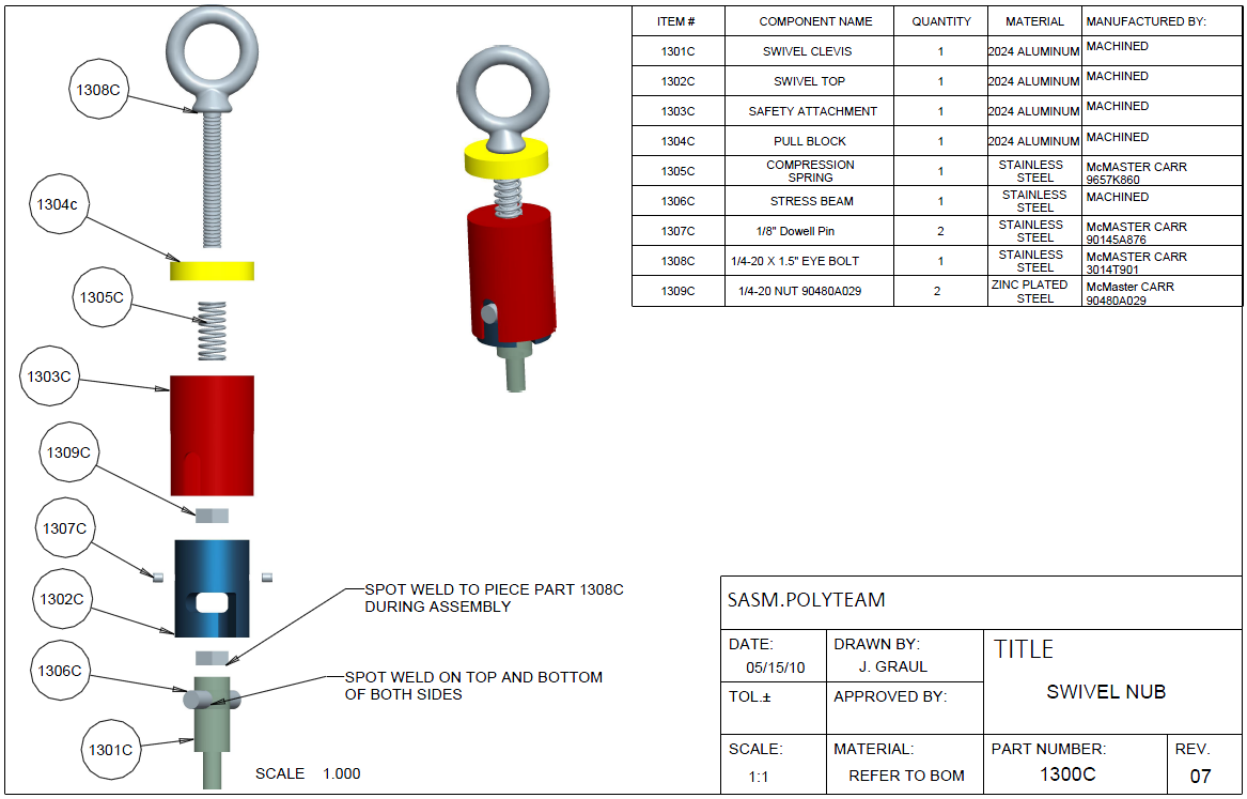

ITEM #	COMPONENT NAME	QUANTITY	MATERIAL	MANUFACTURED BY:
1301C	SWIVEL CLEVIS	1	2024 ALUMINUM	MACHINED
1302C	SWIVEL TOP	1	2024 ALUMINUM	MACHINED
1303C	SAFETY ATTACHMENT	1	2024 ALUMINUM	MACHINED
1304C	PULL BLOCK	1	2024 ALUMINUM	MACHINED
1305C	COMPRESSION SPRING	1	STAINLESS STEEL	McMASTER CARR 9657K860
1306C	STRESS BEAM	1	STAINLESS STEEL	MACHINED
1307C	1/8" Dowell Pin	2	STAINLESS STEEL	McMASTER CARR 90145A876
1308C	1/4-20 X 1.5" EYE BOLT	1	STAINLESS STEEL	McMASTER CARR 3014T901
1309C	1/4-20 NUT 90480A029	2	ZINC PLATED STEEL	McMaster CARR 90480A029

SASM.POLYTEAM			
DATE: 05/15/10	DRAWN BY: J. GRAUL	TITLE: SWIVEL NUB	
TOL.±	APPROVED BY:		
SCALE: 1:1	MATERIAL: REFER TO BOM	PART NUMBER: 1300C	REV. 07

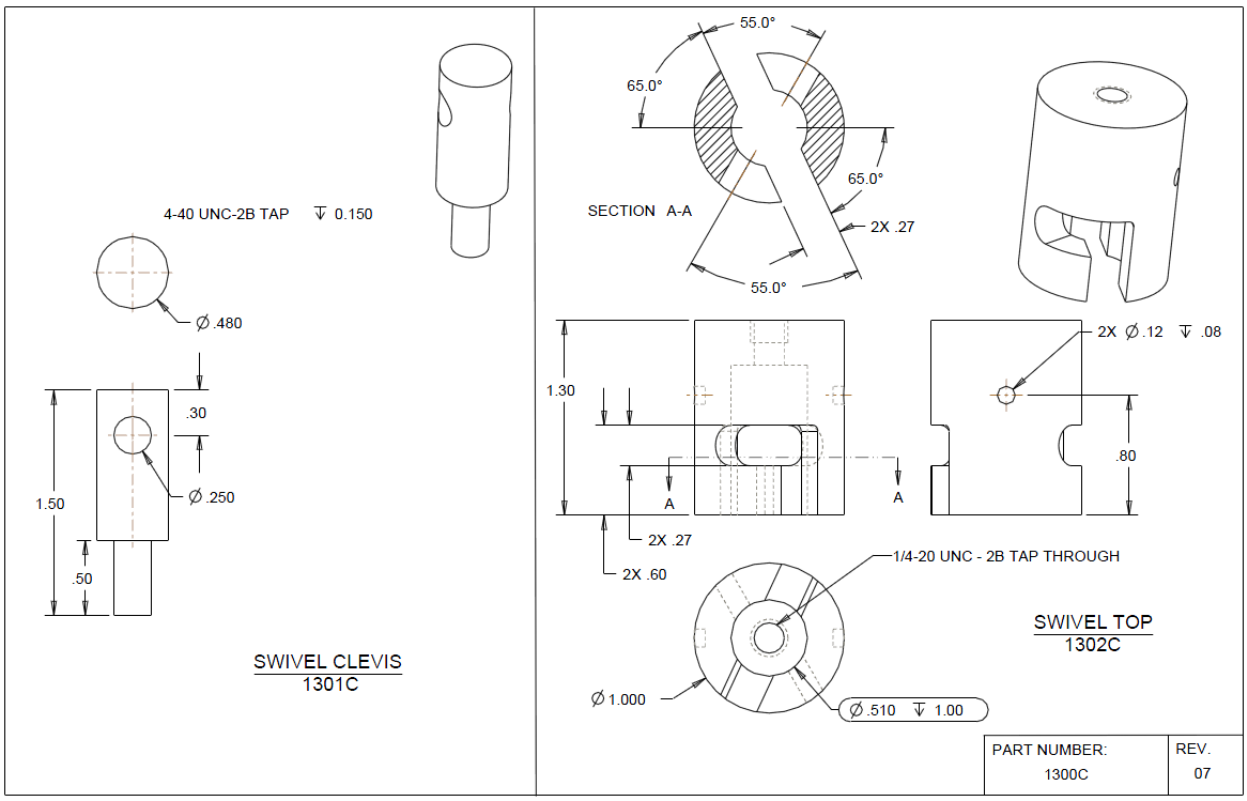

PART NUMBER: 1300C	REV. 07

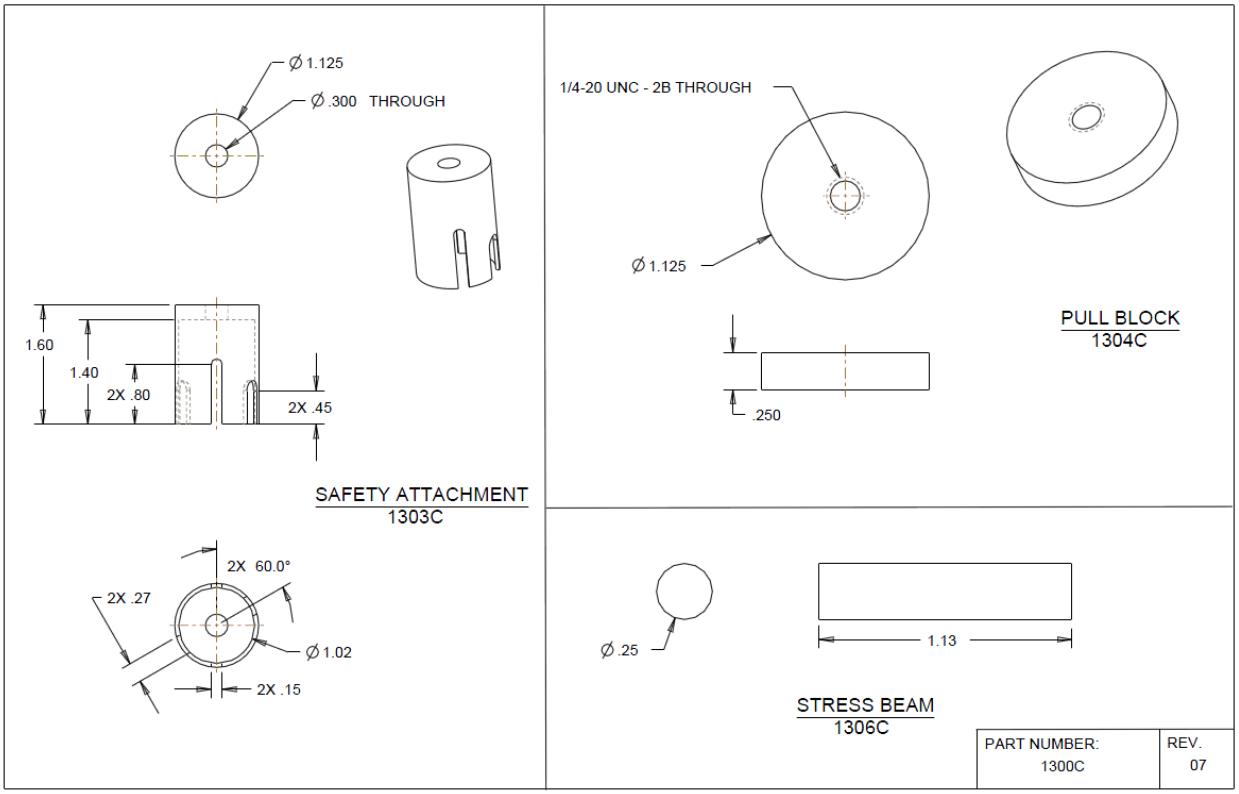
Ø 1.125
Ø .300 THROUGH
1.60
1.40
2X .80
2X .45
SAFETY ATTACHMENT
1303C
2X 60.0°
2X .27
Ø 1.02
2X .15
1/4-20 UNC - 2B THROUGH
Ø 1.125
.250
PULL BLOCK
1304C
Ø .25
1.13
STRESS BEAM
1306C
PART NUMBER:
1300C
REV.
07

Appendix G: Carabiner Stress Analysis

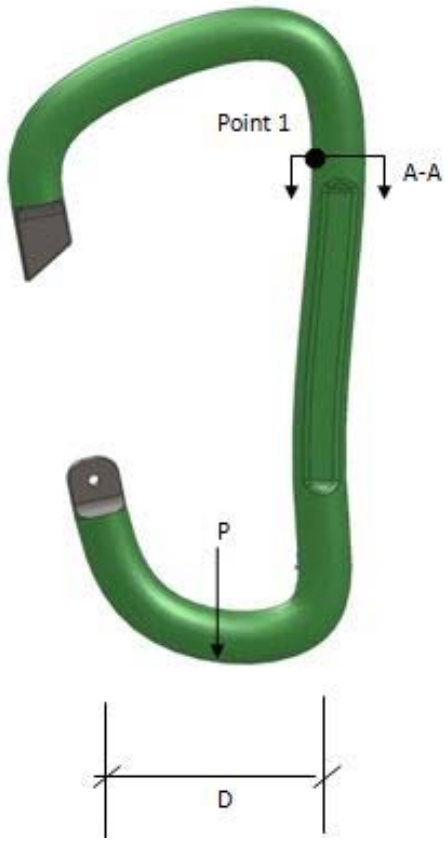

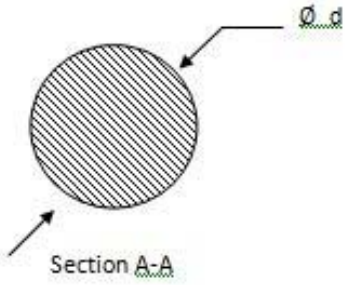

Shear and Bending Distribution

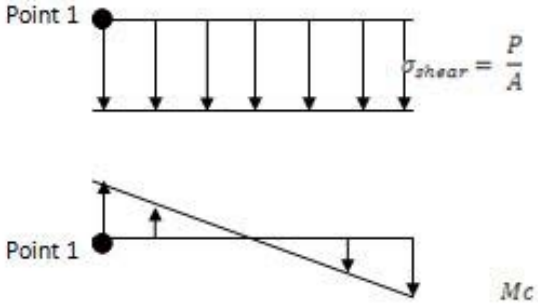

Given:

P=300lbs

d=0.287in (TYP)

D=1.2in (TYP)

Solution:

$$\sigma_1 = \frac{P}{A} + \frac{Mc}{I} = \frac{300}{0.0645} + \frac{137(0.1435)}{0.333 * 10^{-3}} = 63668\ psi$$

$$I = \frac{\pi}{64}(d)^4 = 0.333 * 10^{-3} \quad A = \frac{\pi}{4}(d)^2 = 0.0645in^2 \quad M = \frac{D-d}{2}p = 137in \cdot lbs$$

$$c = \frac{d}{2} = 0.1435in$$

$$\sigma_1 = 63.7\ ksi$$

Appendix H: Pneumatic Stress Analysis

Free body diagram for the analysis of the Pneumatic device

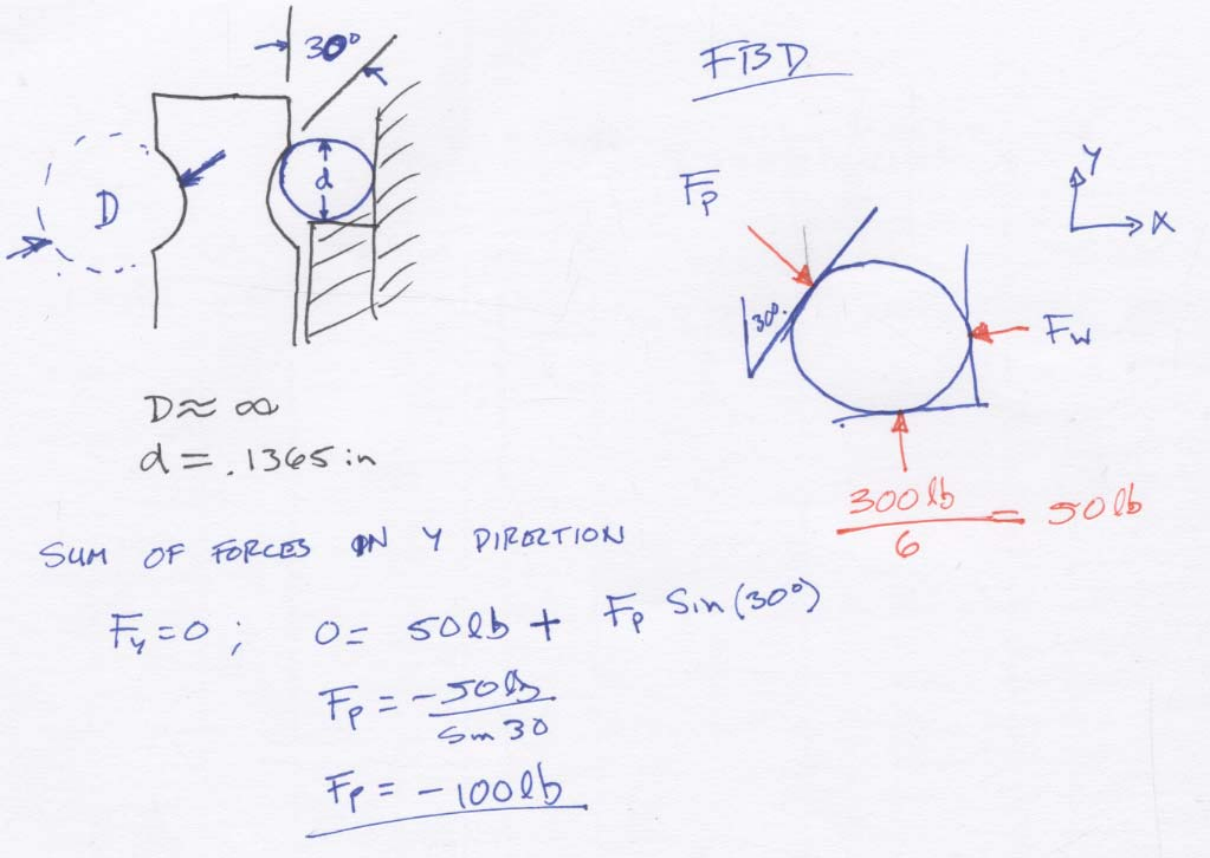

Dimensions and properties

$F = 100$ [lb_f]

$S_f = 30000$ [psi]

$d_1 = 0.1365$ [in]

$d_2 = 1 \times 10^9$ [in]

$E_1 = 3 \times 10^7$ [psi]

$E_2 = E_1$

$v_1 = 0.292$

$v_2 = v_1$

$z = 0.00001$

Stress analysis equations using Engineering Equation Solver (EES)

$$a = \left[\frac{3 \cdot F}{8} \cdot \left(\frac{\frac{1 - v_1^2}{E_1} + \frac{1 - v_2^2}{E_2}}{\frac{1}{d_1} + \frac{1}{d_2}} \right) \right]^{(1/3)}$$

$$p_{max} = \frac{3 \cdot F}{2 \cdot \pi \cdot a^2}$$

$$\sigma_1 = -p_{max} \cdot \left[\left(1 - \frac{z}{a} \cdot \arctan\left[\frac{1}{\frac{z}{a}} \right] \right) \cdot (1 + v_1) - \frac{1}{2 \cdot \left(1 + \frac{z^2}{a^2} \right)} \right]$$

$$\sigma_2 = \sigma_1$$

$$\sigma_3 = \frac{-p_{max}}{1 + \frac{z^2}{a^2}}$$

$$S_y = \left[\frac{(\sigma_1 - \sigma_2)^2 + (\sigma_2 - \sigma_3)^2 + (\sigma_3 - \sigma_1)^2}{2} \right]^{(1/2)}$$

The following are the solutions to the above equations. Notice how the factor of safety (FS) is only .137. Since it is below 1, these calculations indicate it would fail under these stresses.

Unit Settings: [F]/[psia]/[lbm]/[radians]

$a = 0.006784$ [in]	$d_1 = 0.1365$ [in]
$d_2 = 1.000E+09$ [in]	$E_1 = 3.000E+07$ [psi]
$E_2 = 3.000E+07$ [lb_f/in^2]	$F = 100$ [lb_f]
$FS = 0.137$	$p_{max} = 1.037E+06$ [lb_f/in^2]
$\sigma_1 = -818677$ [lb_f/in^2]	$\sigma_2 = -818677$ [lb_f/in^2]
$\sigma_3 = -1.037E+06$ [lb_f/in^2]	$S_f = 30000$ [psi]
$S_y = 218918$ [lb_f/in^2]	$v_1 = 0.292$ [-]
$v_2 = 0.292$ [-]	$z = 0.00001$ [in]

Appendix I: Swivel Nub Stress Analysis

Swivel Top Hand Calculations

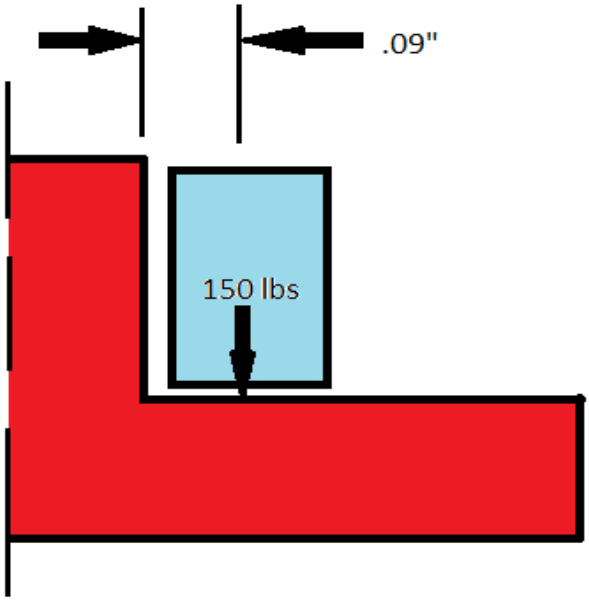

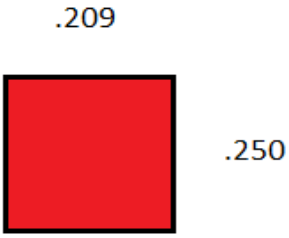

Material Properties of 2011 Aluminum:

$S_y = 47.0Kpsi$

$S_u = 68.0Kpsi$

$$I_x = \frac{bh^3}{12} = \frac{.209in(.25in)^3}{12} = 2.721\times10^{-4}in^4$$

$$M = FD = 150lb\times.09in = 13.5lb\cdot in$$

$$\sigma = \frac{Mc}{I} = \frac{(13.5lb\cdot in)(.125in)}{2.721\times10^{-4}in^4} = 6.2Kpsi$$

$$\tau = \frac{P}{A} = \frac{150lb}{.209in\times.25in} = 2.87Kpsi$$

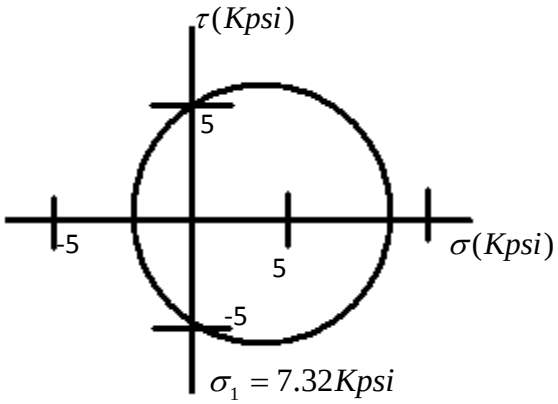

$\sigma_1 = 7.32Kpsi$

$\sigma_3 = -1.12Kpsi$

$$\tau_{Max} = \frac{\sigma_1 - \sigma_3}{2} \geq \frac{S_y}{2n}$$

$$\tau_{Max} = \frac{7.32Kpsi - (-1.12Kpsi)}{2} \geq \frac{47Kpsi}{2n} \qquad n = 5.5$$

Swivel Top Finite Element Analysis

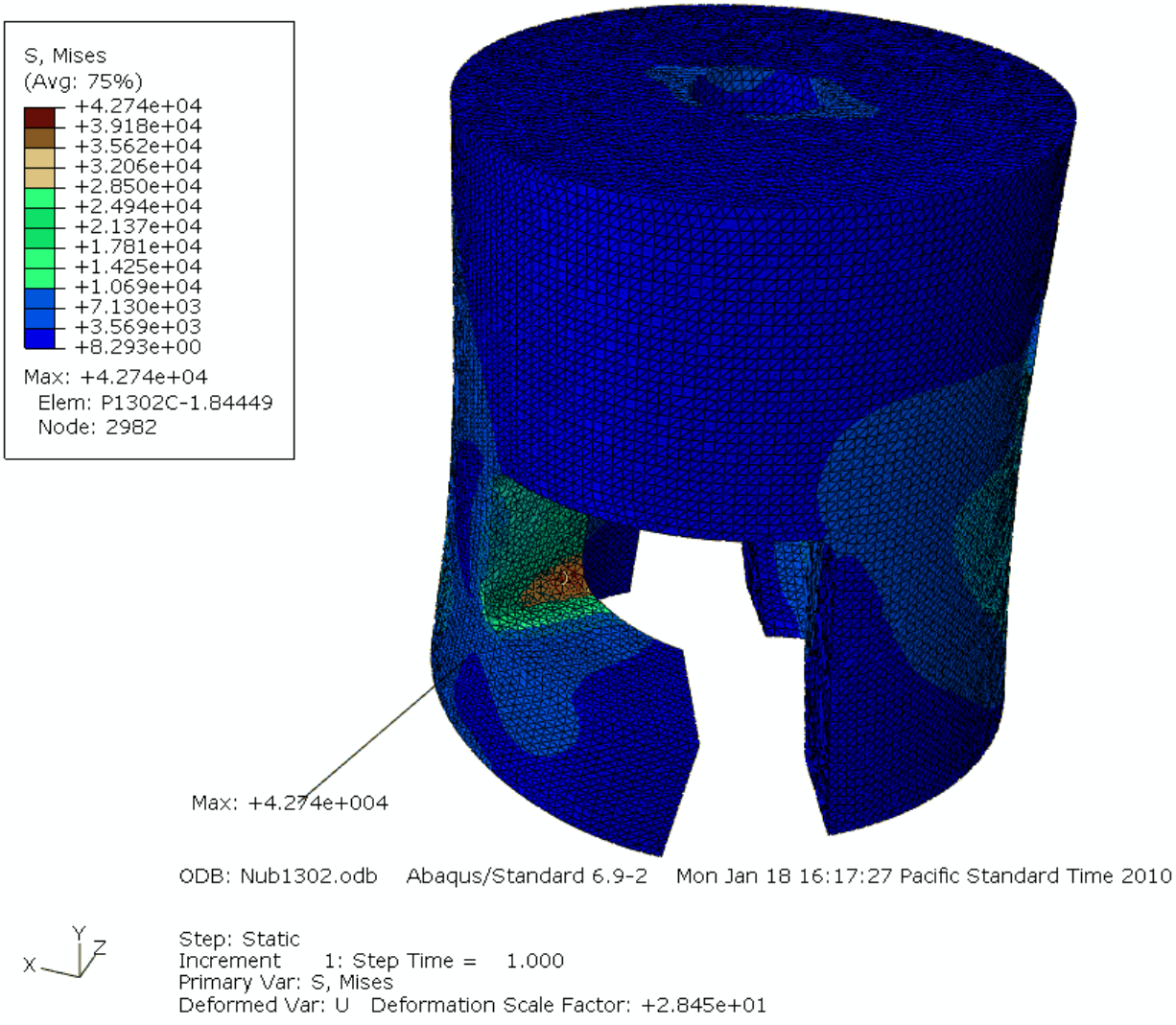

Notes: Analysis #4 was run after Analysis #2 with equal global seed size except for the edges on the 'hook' part and near the max stress concentration. These edges had a Seed biased equal to the seed size of Analysis #3. This was done to provide a continuous mesh convergence. No warnings or errors.

Mesh Convergence:

Analysis #	Elements	Max Stress
1	14009	2.57E+04
2	97180	2.68E+04
4	117447	3.83E+04
3	616234	4.27E+04

Stress Beam Hand Calculations

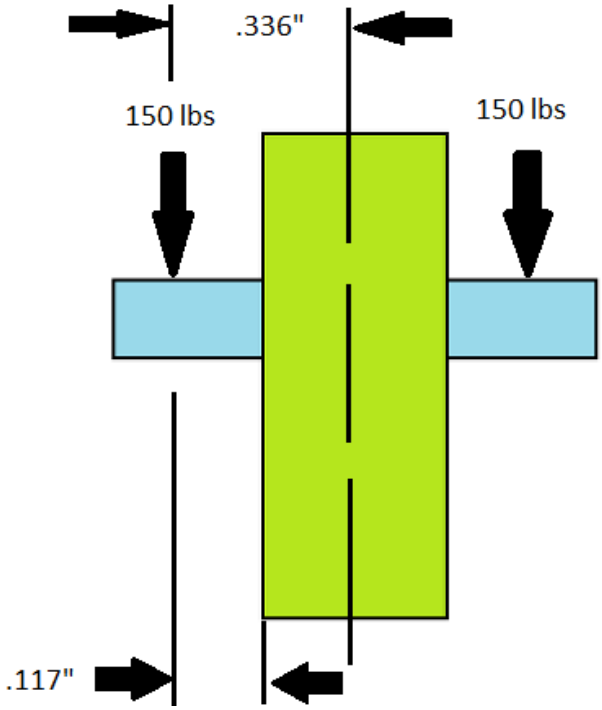

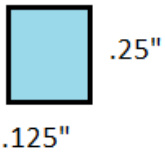

Material Properties of 2024 Aluminum:

$S_y = 24.5Kpsi$

$S_u = 47.0Kpsi$

$$I_x = \frac{bh^3}{12} = \frac{.125in(.25in)^3}{12} = 1.627x10^{-4}in^4$$

$$M = FD = 150lb \times .117in = 17.5lb \cdot in$$

$$\sigma = \frac{Mc}{I} = \frac{(17.5lb \cdot in)(.117in)}{1.627 \times 10^{-4}in^4} = 13.4Kpsi$$

$$\tau = \frac{P}{A} = \frac{150lb}{.125in \times .25in} = 4.8Kpsi$$

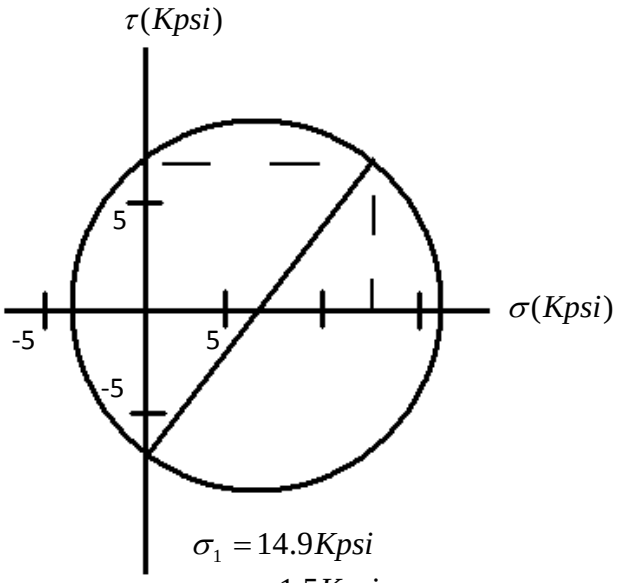

$\sigma_1 = 14.9Kpsi$

$\sigma_3 = -1.5Kpsi$

$$\tau_{Max} = \frac{\sigma_1 - \sigma_3}{2} \geq \frac{S_y}{2n}$$

$$\tau_{Max} = \frac{14.9Kpsi - (-1.5Kpsi)}{2} \geq \frac{47Kpsi}{2n}$$

$n = 2.9$

Stress Beam Finite Element Analysis

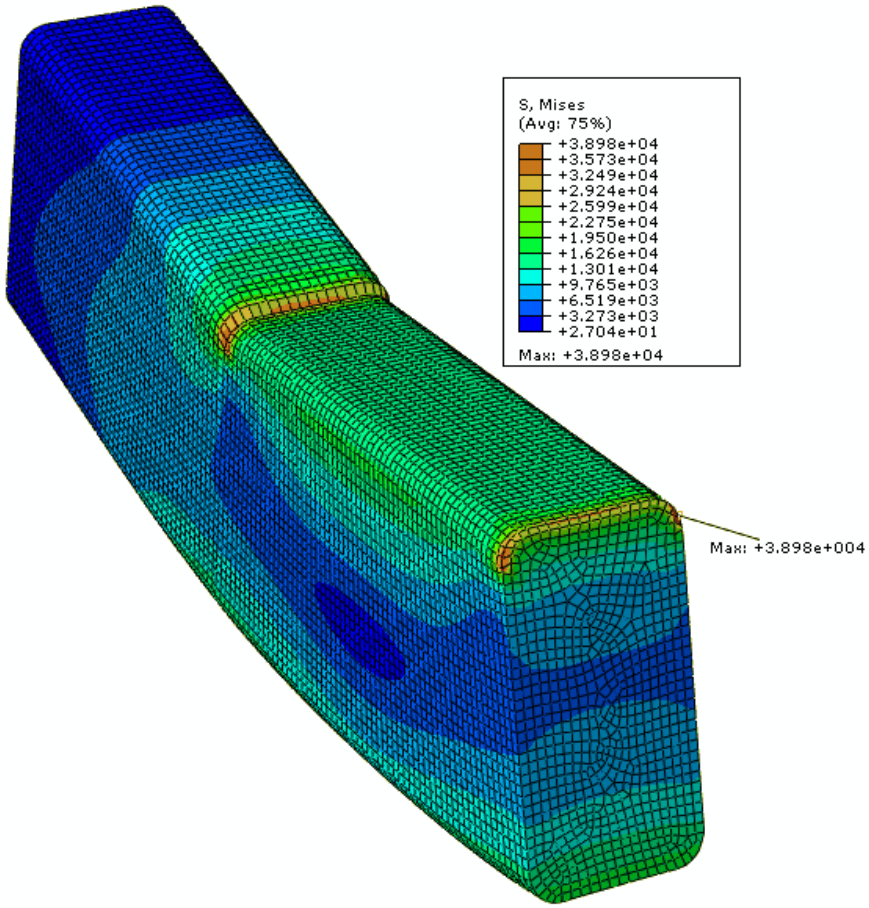

Notes: Shown above is a view of the cross section at the edge of a boundary condition. Quadratic-quadrilateral elements distorted unrealistically around the boundary condition, so all the analysis was done with linear-quadrilateral elements. Further analysis was restricted by computing power. No warnings or errors.

Mesh Convergence:

Analysis #	Elements	Max Stress
1	1950	1.87E+04
2	14480	2.37E+04
3	124000	3.90E+04

Clevis Finite Element Analysis

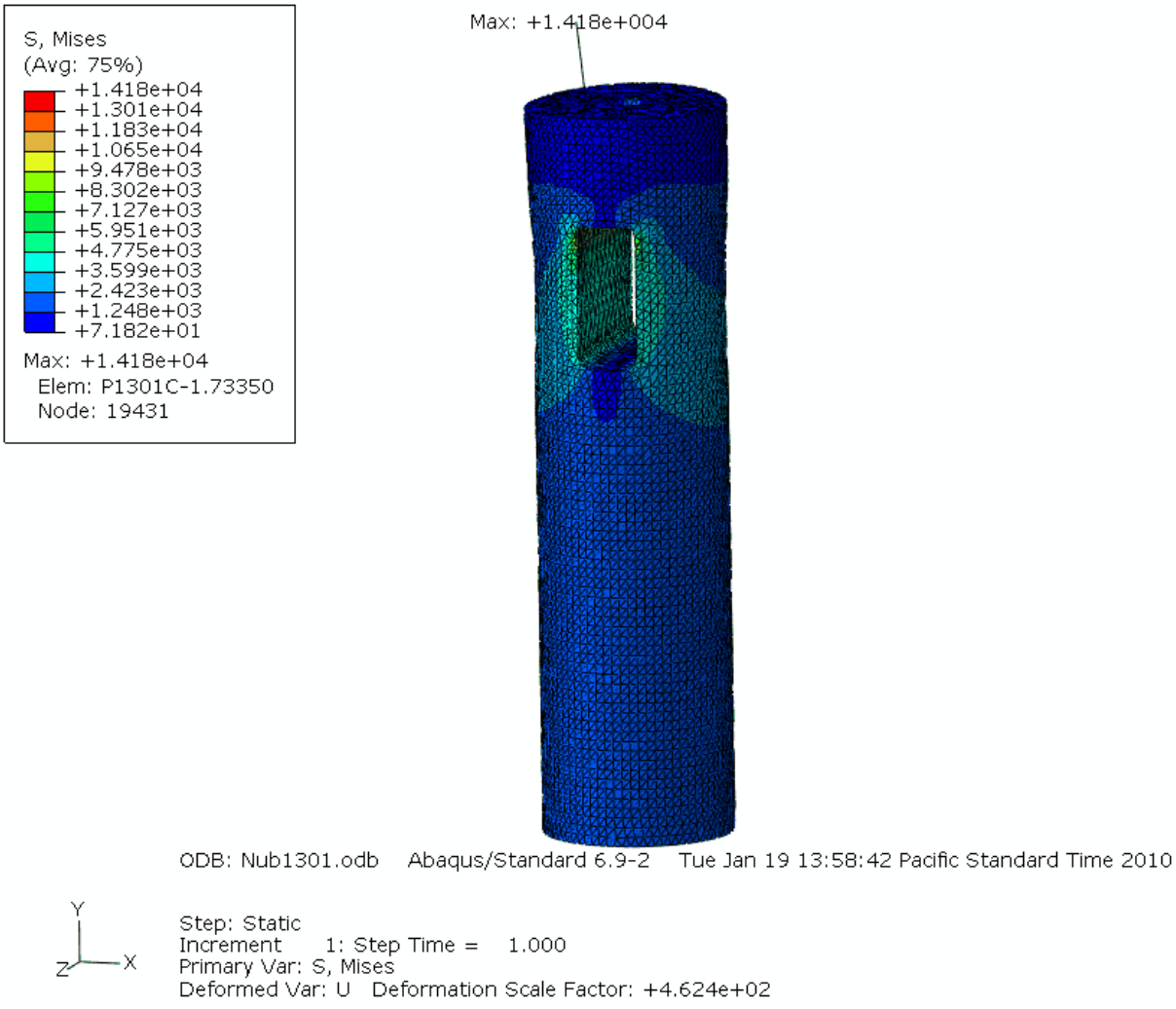

Notes: Consistent results with no warning or errors. No warnings or errors.

Mesh convergence:

Analysis #	Elements	Max Stress
1	27208	1.11E+04
2	138169	1.42E+04

Appendix J: Socket Stud Stress Analysis

Free Body Diagram for the analysis of the Socket Stud

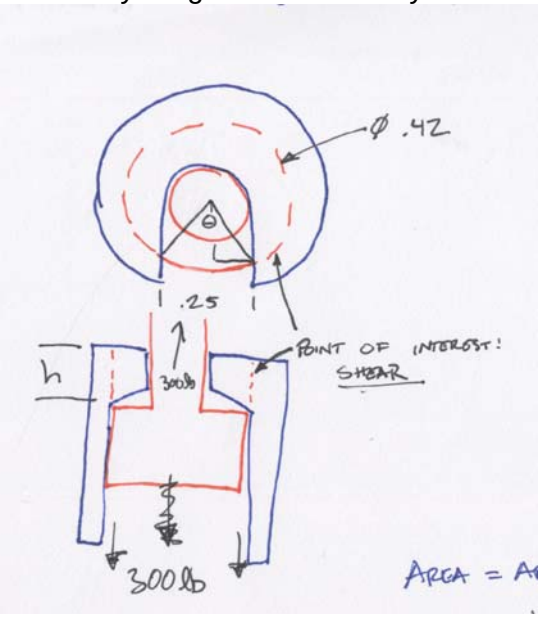

Equations to solve stresses in socket stud using Engineering Equation Solver (EES)

Dimensions and Properties

$F = 300$ [lb_f]

$L_1 = 0.125$ [in]

$H = 0.15$ [in]

$R_1 = 0.21$ [in]

$E_1 = 1.04 \times 10^7$ [psi]

$S_y = 24500$ [psi]

$D_1 = R_1 \cdot 2$ [in]

$D_2 = 0.75$ [in]

Stress Analysis Equations

$$\frac{\theta}{2} = \arcsin\left[\frac{L_1}{R_1}\right]$$

$$L_{arc} = \pi \cdot D_1 \cdot \left[1 - \frac{\theta}{360}\right]$$

$$A_1 = L_{arc} \cdot H$$

$$\tau = \frac{F}{A_1}$$

$$A_2 = 0.5 \cdot \left[\frac{D_2^{\,2}}{4} \cdot \pi - \frac{D_1^{\,2}}{4} \cdot \pi \right]$$

$$\sigma = \frac{F}{A_2}$$

$$\sigma_1 = \frac{\sigma}{2} + \left[\left(\frac{\sigma}{2} \right)^2 + \tau^2 \right]^{(1/2)}$$

$$\sigma_2 = \frac{\sigma}{2} - \left[\left(\frac{\sigma}{2} \right)^2 + \tau^2 \right]^{(1/2)}$$

$$\tau_{max} = \frac{\sigma_1 - \sigma_2}{2}$$

$$\sigma_{von,mises} = (\sigma^2 + 3 \cdot \tau^2)^{0.5}$$

$$SF_{von,mises} = \frac{S_y}{\tau}$$

The following are solutions for the above equations. Notice a safety factor of 12.88

$A_1 = 0.1578$	$A_2 = 0.1516$
$D_1 = 0.42$	$D_2 = 0.75$
$E_1 = 1.040E+07$	$F = 300$
$H = 0.15$	$L_1 = 0.125$
$L_{arc} = 1.052$	$R_1 = 0.21$
$SF_{von,mises} = 12.88$	$\sigma = 1979$
$\sigma_1 = 3133$	$\sigma_2 = -1154$
$\sigma_{von,mises} = 3842$	$S_y = 24500$
$\tau = 1902$	$\tau_{max} = 2144$
$\theta = 73.06$	

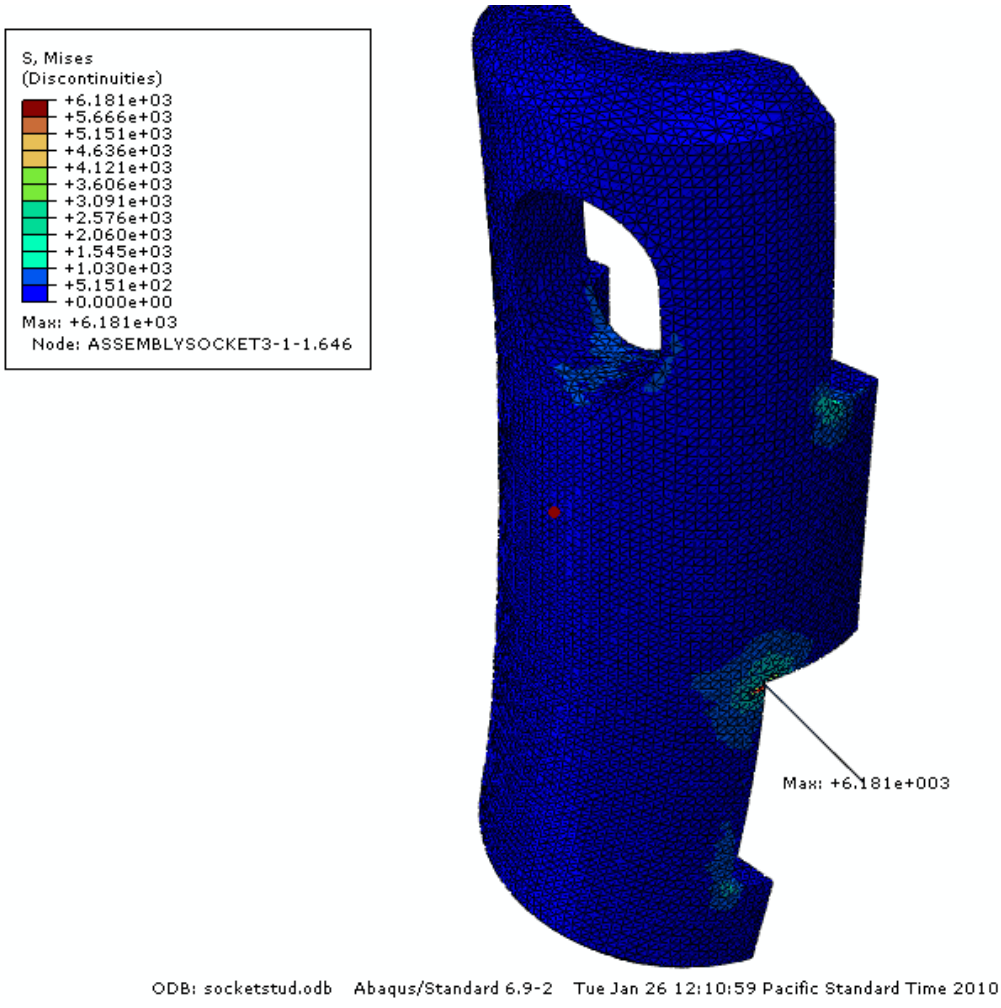

Notes: Max stress occurred at the point of maximum discontinuities with a value of 8.036E3 [psi]. Linear Tetrahedral elements where used for the analysis. There were 10 distorted whose aspect ratio exceeded 0.1. These elements where not located near critical points. Mesh Convergence Shows that there is a 20% change in max stress from analysis 2 to 3.

Mesh Convergence:

Analysis #	Degrees of Freedom	Max Stress
1	3528	6.39E+03
2	18930	6.87E+03
3	122475	8.04E+03

Appendix K: U-Loop Stress Analysis

EES Calculations

Dimensions

$F = 150 \ [lb_f]$

$V = 150 \ [lb_f]$

$b = 0.25 \ [in]$

$b_2 = 0.15 \ [in]$

$h = 0.55 \ [in]$

$r_c = 0.5 \ [in]$

$rad = 0.15 \ [in]$

$d_{pin} = 0.125 \ [in]$

$depth_{bore} = 0.1 \ [in]$

$d_{bore} = 0.265 \ [in]$

Hook Analysis

$$r_o = r_c + \frac{h}{2}$$

$$r_i = r_c - \frac{h}{2}$$

$$c_i = r_n - r_i$$

$$c_o = r_o - r_n$$

$$M = F \cdot r_c$$

$$A_{hook} = b \cdot h$$

$$r_n = \frac{h}{\ln\left[\frac{r_o}{r_i}\right]}$$

$$e = r_c - r_n$$

Stress on Hook

$$\sigma_i = \frac{M \cdot c_i}{A_{hook} \cdot e \cdot r_i} + \frac{F}{A_{hook}}$$

$$\sigma_o = \frac{-M \cdot c_o}{A_{hook} \cdot e \cdot r_o} + \frac{F}{A_{hook}}$$

Shear on Pin

$$A_{pin} = \frac{\pi}{4} \cdot d_{pin}^{\ 2}$$

$$\tau_{max} = \frac{4 \cdot V}{3 \cdot A_{pin}}$$

$$S_{y,pin,min} = 2 \cdot \tau_{max}$$

Stress at Pin on Hook

$$K_t = 1.227 \cdot \left[\frac{d_{pin}}{h}\right]^{-0.935}$$

$$\sigma_{max,pin} = K_t \cdot \left[\frac{F}{(h - d_{pin}) \cdot (b_2 - depth_{bore}) - \left(rad^2 - \pi \cdot \frac{rad^2}{4}\right) + (h - d_{bore}) \cdot depth_{bore}}\right]$$

SOLUTION

Unit Settings: [F]/[psia]/[lbm]/[degrees]

A_{hook} = 0.1375 [in^2]
b = 0.25 [in]
c_i = 0.2217 [in]
$depth_{bore}$ = 0.1 [in]
d_{pin} = 0.125 [in]
F = 150 [lb_f]
K_t = 4.903
rad = 0.15 [in]
r_i = 0.225 [in]
r_o = 0.775 [in]
$\sigma_{max,pin}$ = **16372** [lb_f/in^2]
$S_{y,pin,min}$ = **32595** [lb_f/in^2]
V = 150 [lb_f]

A_{pin} = 0.01227 [in^2]
b_2 = 0.15 [in]
c_o = 0.3303 [in]
d_{bore} = 0.265 [in]
e = 0.05529 [in]
h = 0.55 [in]
M = 75 [lb_f-in]
r_c = 0.5 [in]
r_n = 0.4447 [in]
σ_i = **10724** [lb_f/in^2]
σ_o = **-3113** [lb_f/in^2]
τ_{max} = **16297** [lb_f/in^2]

Appendix L: Coefficient of Thermal Expansion Analysis

The goal of this analysis is to quantify the change in length of the adjustment mechanism and socket stud when placed in series over an extreme temperature difference.

Given:

Coefficient of Thermal Expansion for Steel: $\alpha = 9.6\frac{\mu in}{in \bullet °F}$

Initial Temperature: $T_1 = 25°C \sim 70°F$

Final Temperature: $T_2 = -80°C \sim -112°F$

Active Length of Compression Spring and Socket Stud: $L_0 = 18.385in$

Thermal Strain Analysis:

$$\varepsilon_T = \alpha \Delta T$$

$$\varepsilon_T = 9.6\frac{\mu in}{in \bullet °F} \times \left(-112°F - 70°F\right)$$

$$\varepsilon_T = -.0017472\ \frac{in}{in}$$

$$\varepsilon_T = \frac{L_1 - L_0}{L_0}$$

$$L_1 = (-.0017472\frac{in}{in}) \times 18.3845in + 18.3845in$$

$$L_1 = 18.35239in$$

$$\Delta L = -.032inces$$

Appendix M: Design Failure Modes Effect Analysis

Function	Failure Mode	Potential Effects of Failure	Severity	Cause of Failure	Occurence	Prevention	Detection	Detection Rating	TOTAL
Failure Modes for Adjustment Mechanism									
Adjust Length	Unthreading	Improper Length - Point Loads	6	High weight overcomes friction in thread	4	Locking Mechanism	Manual Inspection	6	144
		Damage to Panels	10	Complete Unthreading	2	Thread stop at end	Visual Inspection	3	60
	Improper setup	Damage to Panels	10	Human Error	3	User Manual	Visual and Manual	3	90
Support	Thermal Expansion	Improper Length	6	Material Properties	2	Protype Builds	Measurement	7	84
		Fracture, Failure	10	Rapid Cooling	4	Maximum Cooling Rate	Visual Inspection	3	120
	Yielding	Payload Damage	10	Overloading	1	Correct Sizing	Spring at max load	6	60
Failure Modes for Quick Connect									
Connection	No Connection	Retry Connection	3	Seizing	5	Maintenance	Does not Connect	6	90
		False Positive Connection	10	Human Error	3	Use safety mechanism	Safety not engaged	3	90
			10	Component Damage	1	Safe Handling	Visible Damage	2	20
	Failure to Disconnect	Disassemble	6	Seizing	5	Maintenance	Does not Disconnect	6	180
Support	Yielding	Payload Damage	10	Overloading	1	Correct Sizing / Material Selection	Spring Failure	3	30
			10	Extreme Temperatures	2	Insulation / Material Selection	Visual Inspection	3	60

Appendix N: Design Verification Plan & Report

Item No	Description	Acceptance Criteria	Measurement	Samples Tested		Results
				Quantity	Date Tested	
1	Unthreading test for adjustment	Vertical height change of ± 1/10 inch	Calipers before and after loading	1	5/9/2010	Adjustment loaded to 300 pounds and no unthreading was observed
2	Thermal cooling test for system	No visible cracks	Microscope at high stress locations	1 each	5/9/2010	Each component was cooled to ~ 70°C and no cracks were observed.
3	Seize test for quick connects	Fully disengage with normal effort	operator (Subjective)	1 each	5/9/2010	Each component was cooled to ~ 70°C and no parts seized during operation
4	Room temperature load test	No material yielding at 300lbs	Calipers before and after 1 full load cycle	1 each	5/9/2010	Each part was loaded to 300 lbs and no failures were observed. Tensile Testing confirmed plastic deformation region in Socket Stud
5	-80 ˚C load test	No material yielding at 300lbs	Calipers before and after 1 full load cycle	1 each	5/9/2010	Each part was loaded to 300 pounds while in the foam container filled with dry ice. No failure were observed.
6	Adjustment Time Testing	< 30 Seconds	Timer	3	5/12/2010	Adjustment from 0 to 30 pounds was able to be done in 8 seconds.
7	Connection Time	<10 Seconds	Timer	3	5/12/2010	Connection of the Stud and Swivel were able to be completed in under 2 seconds.

Appendix O: Expenditure Report

Sub-Assembly		Component / Material	Part Number	Qty.	Actual Cost
Adjustment Mechanism	Compressed Spring Adjustment	Ø1" ID Aluminum 6061 Tube	(MC) 9056K273	3 ft	$35.80
		Ø1" OD x 5" Chrome-Silicon Steel Spring	(MC) 9573K58	3	$23.49
		1-1/16" Internal Retaining Ring	(MC) 91580A216	8	$18.80
		Ø1" Aluminum 2024 Bar	(MC) 8974K133	3 ft	$16.33
		8-32 X5/16 Socket Cap Screw	(HD)	3	$1.00
		1/4-20 Threaded Rod	(MC) 94400A510	3 ft	$9.43
		Ø1/4"-20 Wing Nut Stainless Steel	(HD)	5	$6.76
		E-Ring Style Retaining ring	(MC) 98408A124	25	$5.22
		Ø1/4"-20 Zinc Plated Steel Eye Bolt	(MC) 3014T103	1	$16.22
Quick Connect	Swivel Nub	Ø 1 - 1/8" Aluminum 2024 Alloy	(AS) 03-42250-1	2 ft	$22.42
		1/2" 303 Steel Rod	(MC) 88915K221	1 ft	$15.07
		Ø1/4"-20 Zinc Plated Steel Eye Bolt	(MC) 3014T103	1	$16.22
		Ø1/8" Stainless Steel Dowell Pin	(MC) 90145A469	1	$14.97
		Ø5/16" OD Compression Spring	(MC) 1986K4	1	$11.60
	Socket Stud	Ø1" Aluminum 2024 Rod	(AS) 03-42200-2	3 ft	$24.63
		Ø3/8" OD Compression Spring	(MC) 9657K155	12	$6.58
		1/4-20 X2.5 Socket Cap Screw	(MC) 92196A332	10	$4.89
		1/4-20 Hex Nut	(HD)	3	$1.00
		5/16 Shoulder Screw	(MC) 91829A304	3	$11.01
		Ø1/4 - 28 SHCS	(MC) 92196A332	1	$7.68
Miscellaneous	Swivels and Connectors	1-7/8 Bearing Swivel Eye Clevis	(MC) 8928T13	3	$202.95
		High Strength D Shackel	(MC) 3824T33	5	$52.79
	Tooling	Ø3/16" X 5" Extended-reach Drill Bit	(MC) 28965A735	1	$9.12
		Ø19/64" X 12" Extended-reach Drill Bit	(MC) 2854A35	1	$20.90
		Grooving Tool for Retaining Ring	(MC) 32335A31	1	$31.66
	Testing and Display Fixtures	Lumber	(HD)	-	$25.00
		Hardware	(HD)	-	$70.00
	Shipping	McMaster-Carr & Aircraft Spruce	-	-	$70.00
			Total		$751.54